UNIVERSITY OF CALIFORNIA, SAN DIEGO

Robotic Removal and Introduction of a Mechanical Attachment on the Surface of Mars

A Thesis submitted in partial satisfaction of the requirements

for the degree Master of Science

in

Engineering Sciences (Aerospace Engineering)

by

John Thomas Cale Davis

Committee in charge:

Professor David J. Benson, Chair
Professor Frank E. Talke
Professor Hidenori Murakami

2013

The Thesis of John Thomas Cale Davis is approved, and it is acceptable in quality and form for publication on microfilm and electronically.

_____

_____

_____

Chair

University of California, San Diego

2013

DEDICATION

I found this section to be the most difficult and therefore final section that I completed. I bounced around from dedicating to all of those mentioned in my acknowledgement section. However, none of these other events in my life would have happened without my dad stressing the importance of education, so I would like to dedicate this thesis on his behalf.

Figure 1 - Father-Son Indian Guide Trip, Circa 1987

EPIGRAPH

"Astronomy compels the soul to look upward, and leads us from this world to another."

— *Plato,* The Republic*, 342 BCE.*

"Wild waves of the sea, casting up the foam of their own shame; wandering stars, for whom the gloom of utter darkness has been reserved forever."

— *(Jude 1:13)*

"The logistic requirements for a large, elaborate mission to Mars are no greater than those for a minor military operation extending over a limited theatre of war."

— Wernher von Braun, The Mars Project, written in German in 1948, published as "Das Marsprojekt" in 1952, first English edition published in 1953.

TABLE OF CONTENTS

LIST OF ABBREVIATIONS

CAD	Computer Aided Design
FEA	Finite Element Analysis
JPL	Jet Propulsion Laboratory
MSL	Mars Science Laboratory
NASA	National Aeronautics and Space Administration
UCSD	University of California, San Diego
DBA	Drill Bit Assembly
MPa	Mega-Pascal

LIST OF FIGURES

LIST OF TABLES

LIST OF GRAPHS

PREFACE

While the work contained within this thesis was not done as research at UC San Diego, I do attribute it to the knowledge and skills that I learned while a student within the University.

I finished the 2 year program in a year and a quarter. In what would be my final quarter, I attended the Triton Fall Science and Technology job fair. I spoke with a recruiter and then two senior-level engineers from NASA-JPL and was invited to a second interview onsite in Pasadena. Not expecting it to be much more than a learning experience I went and they liked my enthusiasm toward Computer Aided Design. I was offered a position that same day. It was a surprising and unreal feeling. I asked them if I could finish my degree as I was in my final quarter to which they replied "absolutely". However, upon finishing my coursework in December 2006, my wife and I moved up to the Los Angeles area and I began working.

Fast forwarding now almost 5 years, I was fortunate enough to get to work on a number of space missions including most notably the MSL Rover. While working at JPL, I have always felt that I should complete my

Masters of Science degree at UC San Diego. I am thrilled to be given the opportunity to submit this Master's thesis that covers some of the advanced design and engineering analysis that I performed while working on the Mars Rover project at the Jet Propulsion Laboratory in Pasadena.

My route from a beginning graduate student to the completion of my Master's degree has been both lengthy and circuitous, I feel fortunate to have been presented the opportunities, both academically as well as professionally, to learn and apply my knowledge to a practical problem. This thesis is a perfect way to combine theory and application.

VITA

2002	Associates of Arts – Mathematics El Camino College
2005	Bachelor of Arts – Aerospace Engineering University of California, San Diego
2006	Engineer-In-Training (EIT) Board for Professional Engineers and Land Surveyors
2007	Master of Business Administration – Project Management American Intercontinental University
2013	Master of Science – Aerospace Engineering University of California, San Diego

ACKNOWLEDGEMENTS

I would like to acknowledge all those that helped me in completing this thesis, beginning with my mom and dad, Susan and Glenn Davis for raising me and providing me with all of the opportunities that they could. My siblings, Mary, Mitch, and Steven, as well who were always willing to play with Lego's with me.

I also would like to acknowledge my wife, Nokomas, who I met while a student at UC San Diego, and my son, Kai'Ani Ora, who was born during my time as a graduate student. Also very instrumental in my life were my three best friends, Chirs Ioimo, James Petitfils, and Ryan Sholty who really I consider more of family than friend. Their wives and children I would also like to acknowledge as their relationships have proven invaluable for me in my own relationship.

I would also like to acknowledge several teachers and professors that have stood out in my education. Mr. Bruckner, who in 1st grade both pushed me into 2nd grade math classes and helped me with my first "girlfriend." Mr. Baumgartner in high school that showed me it was ok to be both good at math and "cool" at the same time. Mr. Leonardo at El

Camino CC who taught me physics and to this day taught in the most honest and understandable way. To most recently Professor Talke, who both introduced me to computer-aided design, which is now my profession as a mechanical design engineer, and oversaw the completion of my thesis and corresponding master's degree.

ABSTRACT OF THE THESIS

Robotic Removal and Introduction of a Mechanical Attachment on the Surface of Mars

by

John Thomas Cale Davis

Master of Science in Engineering Sciences (Aerospace Engineering)

University of California, San Diego, 2013

Professor David J. Benson, Chair

This thesis details the mechanical design and analysis of the MSL BitBox, which allows the robotic arm of a specially designed Mars rover to replace a drill bit assembly that is attached to the robotic arm with an identical back-up. This is all accomplished though built-in functionality of the robotic arm along with additional mechanisms of the BitBox. The

thesis begins by providing an overview of the BitBox and then moves into detailing the design of the components. Then a presentation of the finite element analysis utilized to refine the design is discussed. Finally, the thesis provides an overview of the operation of the BitBox and its interaction with the MSL Rover's robotic arm. The resulting design proved to be very functional, and two BitBoxes were implemented rather than one as originally planned. Variations of the BitBox design could be used for other rover missions that utilize a robotic arm, both on terrestrial planets as well as in deep-sea operations.

CHAPTER I: INTRODUCTION

In all of previous rover missions to Mars, there had never been a way to introduce a new attachment to the robotic arm once the rover had landed. However the arm was assembled on Earth, is how it was to be used on Mars. This simplified the function of the robotic arm, but limited its capabilities should a modification need to be made. Due to the five time increase in length of the mission for the Mars Science Laboratory (MSL) Rover, and the ten time increase in the number of samples that it is capable of taking, it was deemed that there needed to be a way to replace the drill bit assembly with a replacement, should that need come about.

1.1 BITBOX

The BitBox was designed with only the mounting interface locations on the MSL Rover defined. The BitBoxes also had to be within the range of motion of the robotic arm so they were able to be accessed properly. The final requirement was that it had to work with the current design of the drill bit assembly as they had already been fabricated and assembled.

The resulting design of the BitBox is shown in Figure 2 with a drill bit assembly, on the right of the picture, retained within.

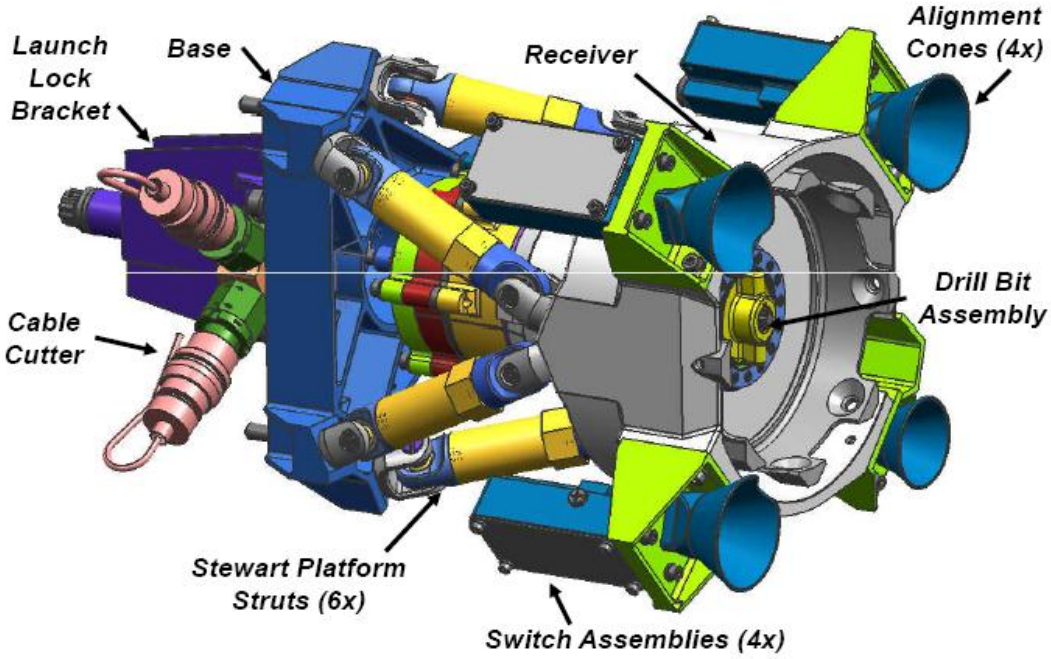

Figure 2 – BitBox Assembly, CAD Model

This entire design, analysis, and assembly was done at JPL, and some of the fabrication as well. I was designated to be on a three-member "tiger team" tasked with turning this into a functioning assembly. My role on the team was three-pronged. First, I had to conceptualize the mechanisms required to obtain the functionality with another engineer on the team. This includes the auto-aligning of the BitBox to the robotic arm, the retaining and releasing system for the drill bot assembly, and launch-

locking the assembly in place until it land on the Martian surface. Second was the complete design and drafting of all of the parts in a CAD environment. Third was to optimize the design using finite element analysis to ensure strength requirements were met while minimizing the weight of the assembly.

The mechanisms co-conspirator on the team was also responsible for the manufacturing of the parts, assembling them to JPL standards and ensuring the other subsystems of MSL were not negatively affected by our addition.

The third team member was responsible for the electronic and software implementation as well as testing and analyzing the assembly prior to mounting them onto the rover.

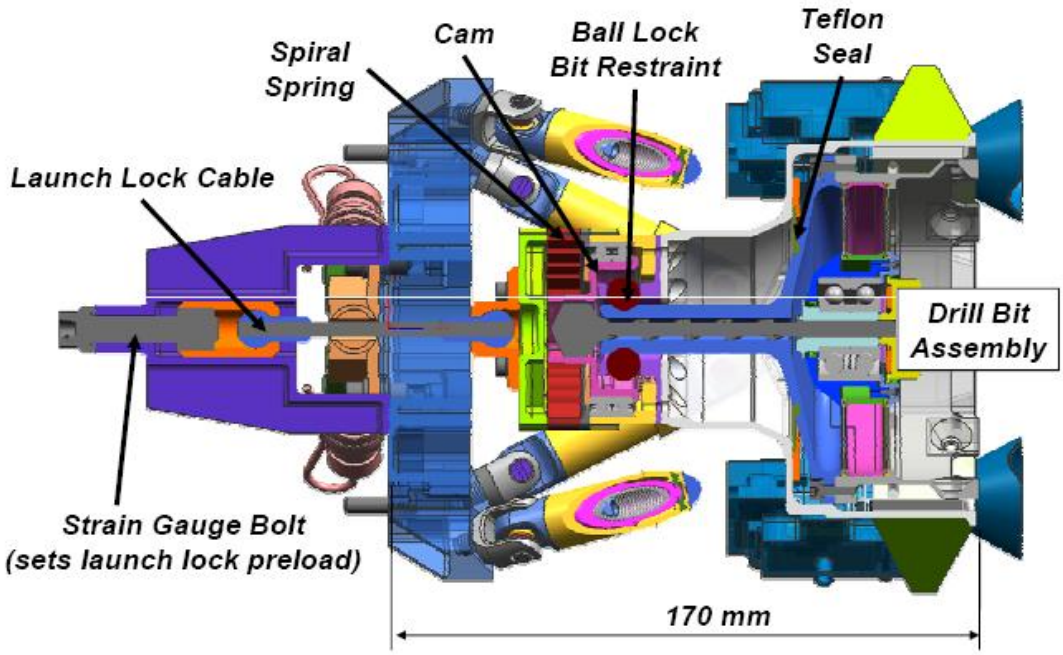

Figure 3 – BitBox Assembly, CAD Model Section View

Figure 3 shows the interior components of the BitBox and some of the mechanical features and mechanisms that are being used for this assembly.

1.2 DRILL BIT ASSEMBLY

The purpose of the two BitBoxes are to provide the MSL Rover the ability to exchange drill bits on the surface of Mars in case the in-use drill bit becomes damaged or inoperational. The process is similar to that of exchanging a drill bit on any hand-held drill, the difference being that this all has to be done remotely so the clamping force must be provided mechanically. The drill bit assembly is also far more complex than a hand-held drill in that is also captures the drilled material to be sampled and analyzed. The drill bit assembly is shown in Figure 4 and it is this entire assembly in the picture that is to be removed and replaced.

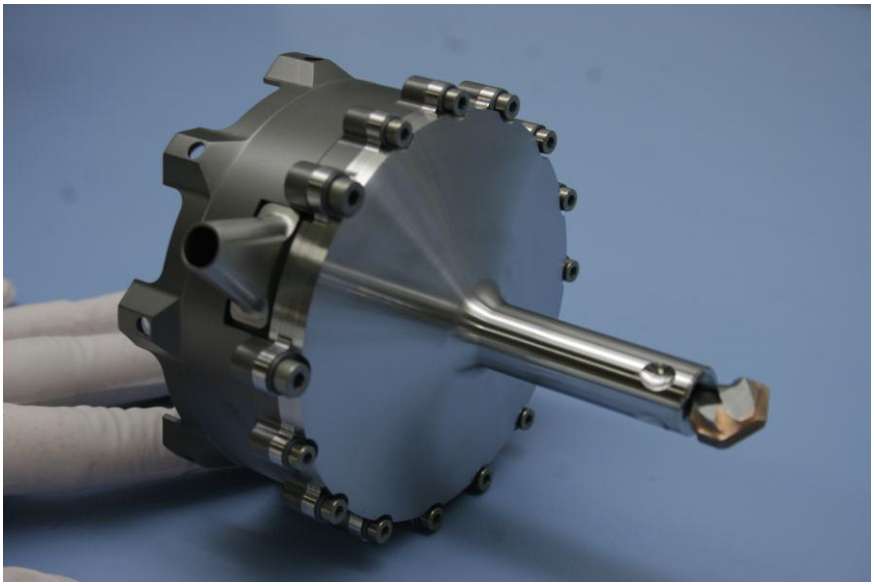

Figure 4 - MSL Drill Bit Assembly

1.3 LOCATION ON MSL ROVER

The location of the BitBoxes on MSL is on the front panel, which is also where the robotic arm is mounted. In order to be accessible by the robotic arm, the two BitBoxes cannot be mounted directly to the panel but must be cantilevered away from it and also each must be angled in a different direction. Figure 5 shows the two BitBoxes mounted to the Rover front panel.

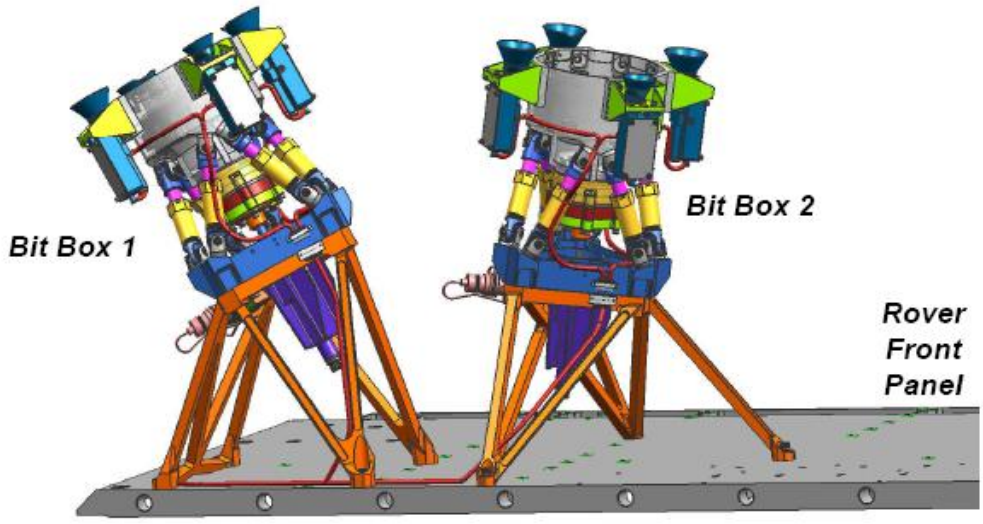

Figure 5 – BitBox Locations on Front Panel of MSL Rover

The following figures 6 and 7 below shows a 3-D CAD front view of the MSL Rover with the two BitBoxes in their location beneath the robotic arm, followed by the actual BitBoxes installed on the MSL Rover.

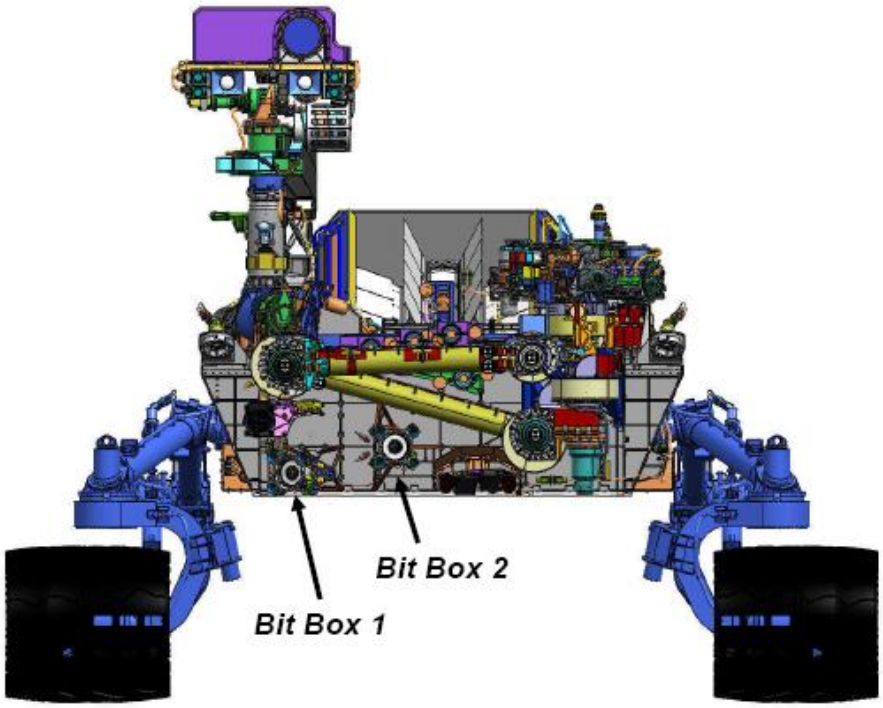

Figure 6 – Front View of MSL Rover, CAD Model

Figure 7 – Front View of MSL Rover

Figure 8 shows the installation of the BitBox to the front panel of the Rover.

A torque gauge is used to not over-torque the fasteners.

Figure 8 – Installation of BitBoxes onto MSL Rover

CHAPTER II: COMPONENT DESIGN

2.1 OVERVIEW

In thinking about the functionality that was required of the BitBox, several conceptual designs were created in CAD to better understand the pros and cons of each assembly design. This began with a simplistic barrel design that held the drill bit assembly snugly and was affixed to the front panel of the MSL Rover. However, the robotic arm could come at the BitBoxes out of angle by 2 degrees so there needed to be some sort of "auto-align" feature built into the BitBox that adjusted the angle of the drill bit assembly to match that of the incoming robotic arm. The solution was to have part of the BitBox be hard mounted to the front panel of the rover while a second part of the BitBox held the drill bit assembly and was kinematically attached to the fixed part of the BitBox. Another way to think about this is the part that is directly mounted to the rover is called the fixed-plate while the part that is stood off from the front panel is called the free-plate. The free-plate is connected to the fixed-plate by linkages that allow motion of the free-plate to allow the auto-aligning to the robotic arm.

In robotics there is just such a device that is currently used in the market. It is a hexapod structure known as a Stewart Platform. It is a type of parallel manipulator that incorporates six linear actuators to give the free-plate full range of motion in all six degrees of freedom. The Stewart platform is most notably used in flight simulators, but also is common in telescopes, PCB manufacturing, and CNC milling machines.

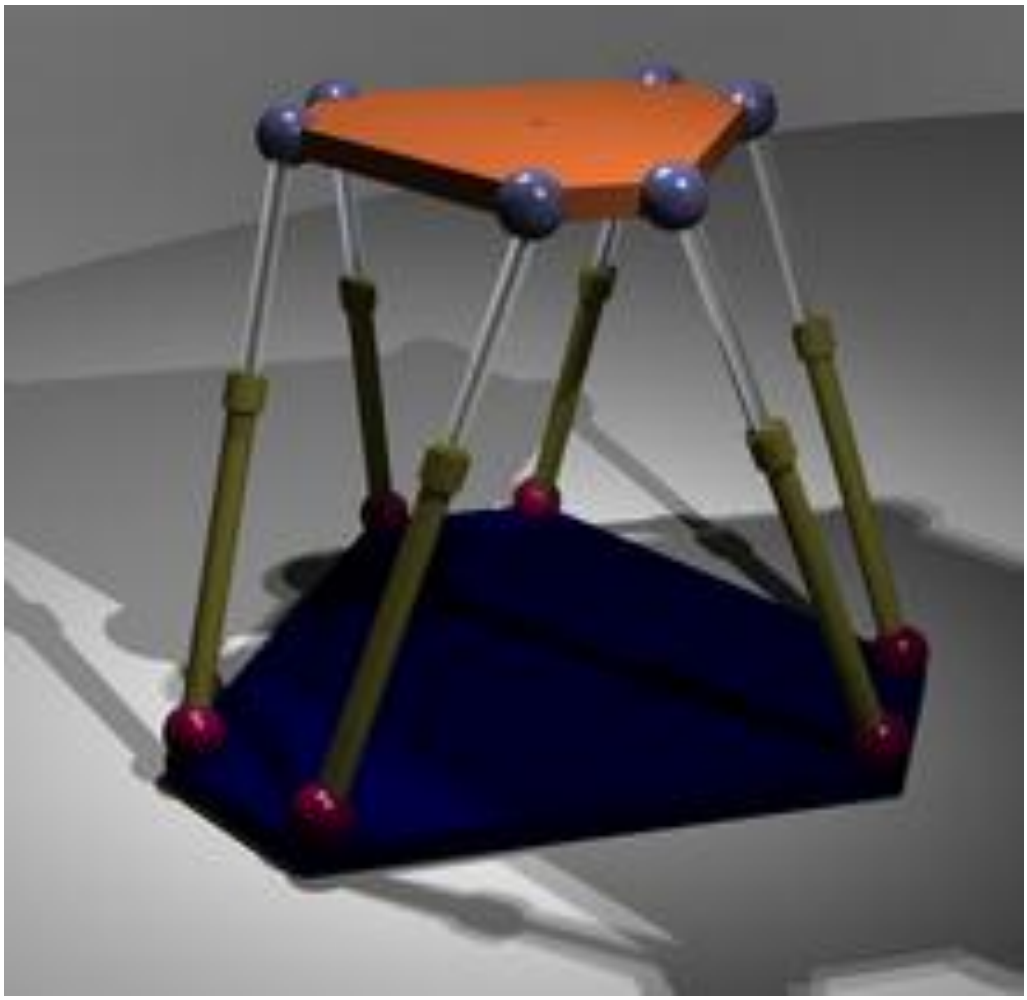

Figure 9 - Stewart Platform Conceptual Design

Figure 9 shows the typical geometric arrangements of a Stewart Platform where the bottom plate is the fixed-plate and the top plate is the free-plate. While this Stewart Platform mechanism was the basis for the design, there was still much work to be completed on the actual BitBox version of the Stewart Platform.

2.2 BASEPLATE ASSEMBLY

The main structure to which the struts mount is the fixed-plate of the Stewart Platform. This part was renamed to be the baseplate for the MSL BitBox, but its function is identical to that of the aforementioned fixed-plate. This is shown if Figure 10 as a baseplate with the 6 struts.

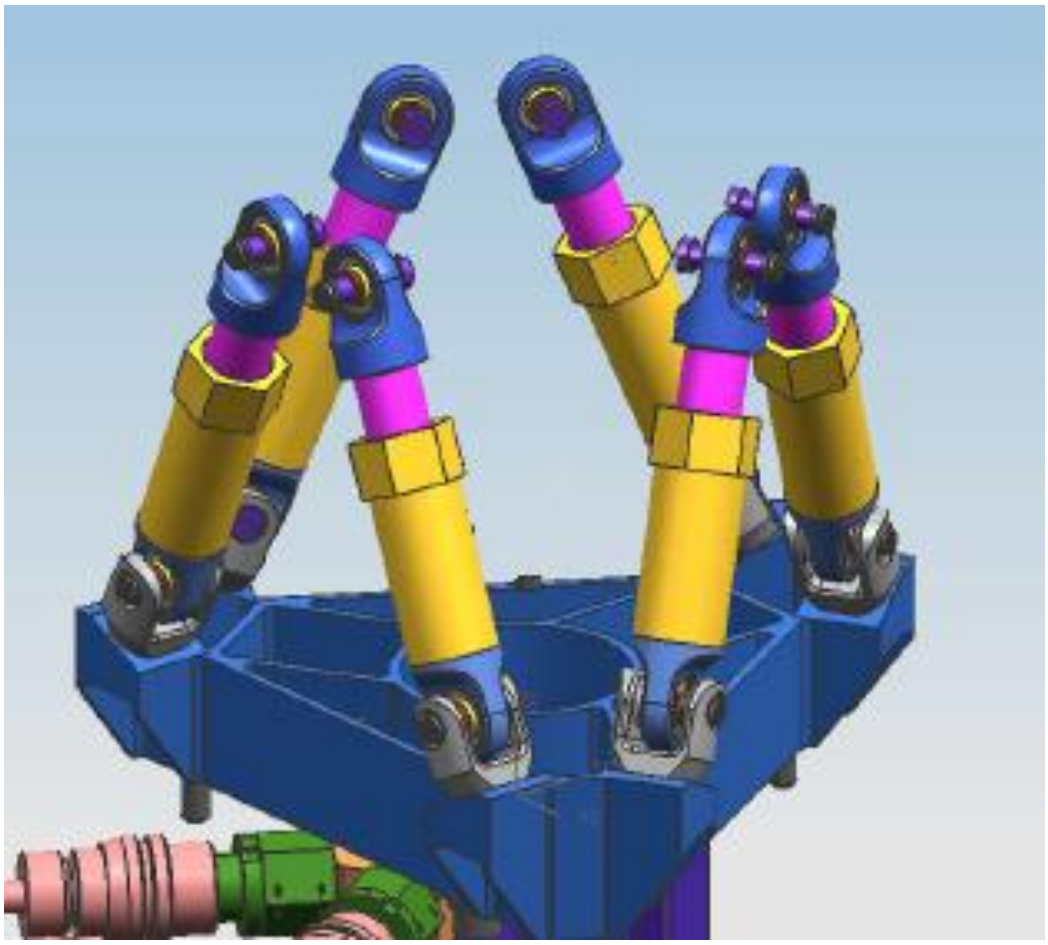

Figure 10 - BitBox, Struts on Baseplate

It is designed to mount the BitBox struts on one side through the use of pins and clevises mounted on the baseplate, and also the launch-lock assembly (detailed in section 2.7) on the opposite side. The initial the design was to be a 1:1 hexapod which implies that the fixed-plate and free-plate have the same diameter. However, during MatLab iterations, the design was changed to a 5:4 hexapod. This difference was allowable as the spherical bearings in the struts would easily accommodate this and still have their full travel available to them.

2.3 STRUT ASSEMBLY

With the geometrical design of the Stewart Platform now iteratively optimized in MatLab, the strut detailed design could now commence. Again, there were limitations of the length predetermined by the fixed and free plates of the Stewart Platform and the MatLab analysis also dictated that the stroke length of the struts was to be 11.2mm. Figure 11 shows the extended and compressed configurations of the struts at the limits of the stroke.

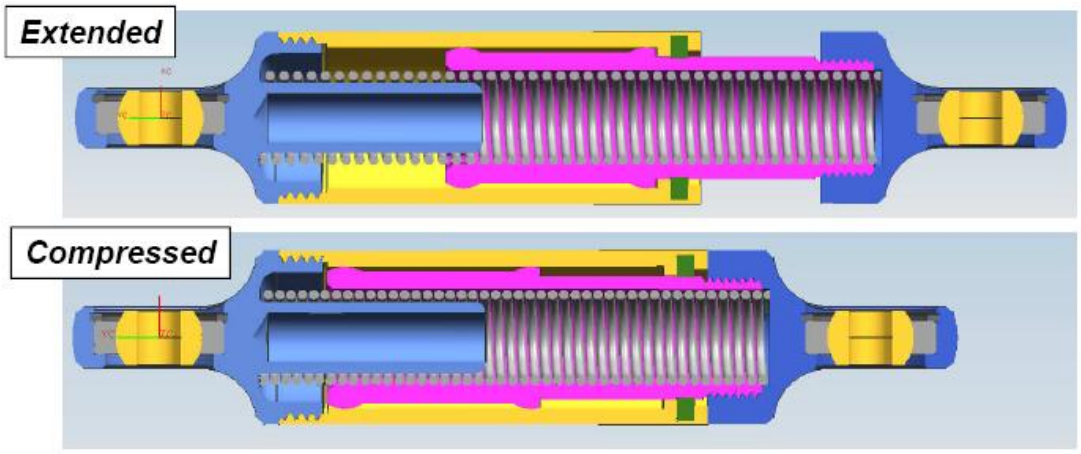

Figure 11 - BitBox Strut, Range of Motion

The struts also had to be able to support the weight of the free-plate of the BitBox which hold the drill bit assembly. To accomplish this, the struts had to have their internal spring be preloaded to a point where rigidity

was maintained and linear actuation would only occur when acted upon by the robotic arm. This preload of the springs, in order to have the BitBox remain rigidly suspended, was calculated to be 19.4 Newtons. Having the BitBox in a cantilevered position really worked against us in the design of this as the springs were required to be preloaded a considerable amount, in fact over 50% of the free length of the spring. Figure 12 shows the 3 configurations of the spring.

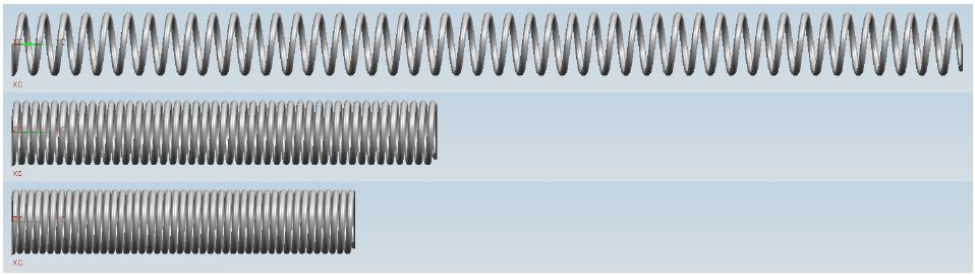

Figure 12 - Strut Spring, Working Lengths

At top is the free length of the spring, while in the middle is the preloaded length (when the strut is free), and at bottom is the compressed length (when the strut is fully compressed). The difference in length between the middle and bottom spring representations of the spring is the 11.2mm. The first pass of the spring design we started with the free length of the spring and worked forward to the preloaded and then compressed configurations. However, we quickly realized that the coils were

overlapping in that they needed to compress so much to reach the expectations of the struts. So in order to achieve these design goals, the spring was going to need to have a long displacement when using Hooke's Law. Therefore we had to work backward, beginning with the fully compressed configuration, leaving a quarter coil diameter between coils, and working out to the free length of the spring. This proved to be the more appropriate way to go and the ideal spring constant, k, was thereby found to be 0.27 N/mm.

With this key mechanical component of the strut now determined, the rest of the strut could be designed around the spring. Figure 13 details all of the parts that constitute the strut.

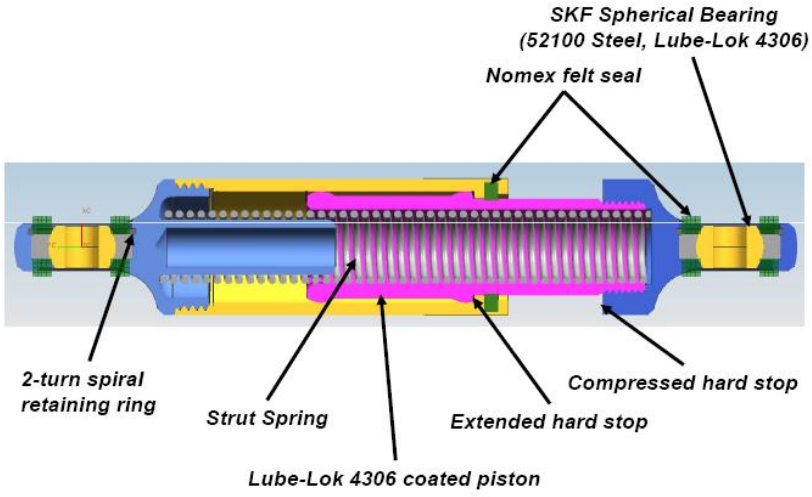

Figure 13 - Components, BitBox Strut

The strut spring can be seen as the centerpiece of the part. The spring is compressed and preloaded by the two end caps. These end caps also house a spherical bearing which allows the rotational motion of the BitBox. The spring is retained within the bore and piston of the strut which allows for the linear motion of the BitBox. Finally, to keep dust particulate out of the moving surfaces, of the spherical bearings and the stroke of the strut, Nomex felt seals were places in these critical areas. Figure 14 below shows the fabricated and anodized end caps, bore and piston of the strut.

Figure 14 - Fabricated Strut Components

Figures 15 and 16 show the assembled strut assembly at its two operational limits.

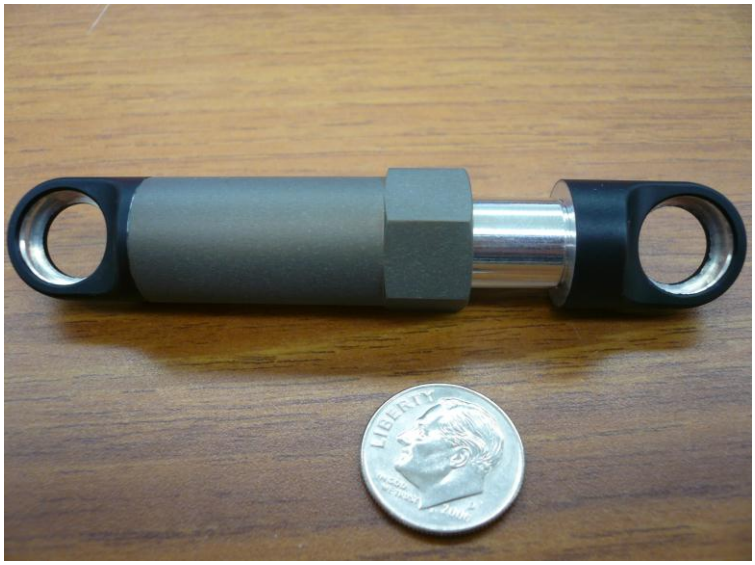

Figure 15 – Strut Assembly, Free Position

Figure 16 – Strut Assembly, Compressed Position

2.4 RECEIVER ASSEMBLY

The receiver assembly is what combines all of the aspects detailed by the design drivers into one central meeting point

2.4.1 BITBOX RECEIVER

The main part of the receiver assembly is the BitBox receiver, shown in the Figure 17.

-

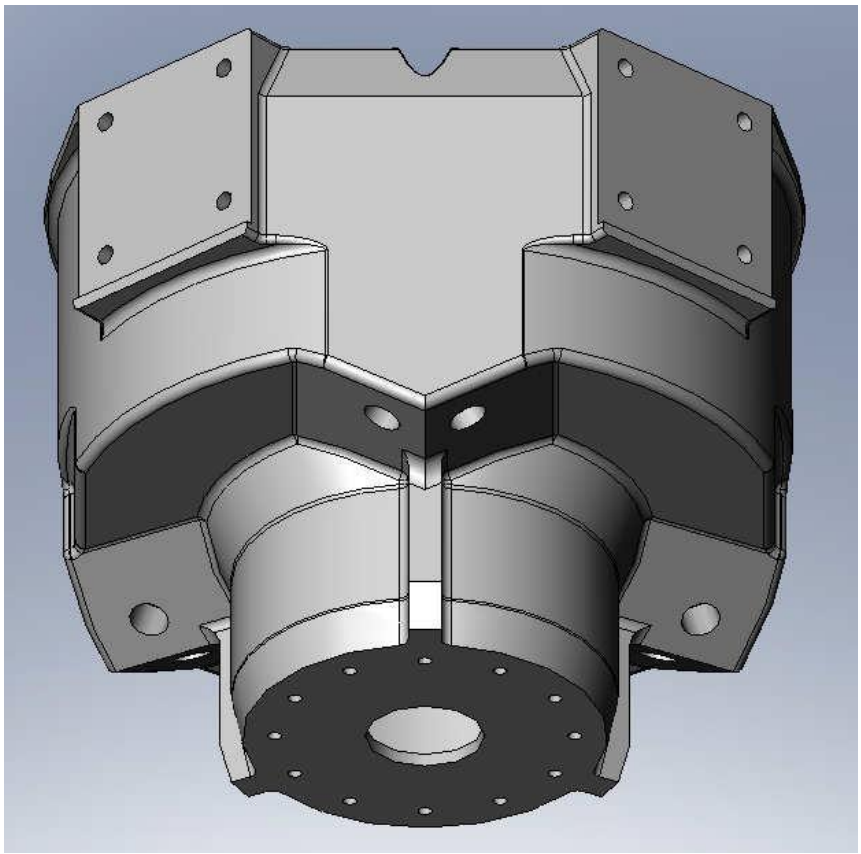

Figure 17 - BitBox Receiver

This part is both the free-plate of the Stewart Platform design for the MSL BitBox as well as being responsible for retaining the replacement drill bit assembly.

Due to the complexities of the BitBox, the design of the BitBox receiver part morphed from a simple cylinder to the multifaceted part that was shown in the previous figure. Starting with the two square pads at the top left and top right, these are used to mount the brackets that hold the alignment cones and micro-switch assemblies that are detailed in the next section. There are a total of four of these equally spaced around the perimeter of the receiver. Between these pads there is another flat surface and is a guide feature for the robotic arm to detect and then slide along as it engages the BitBox to acquire a replacement drill bit assembly. Below these pads there are mount surfaces shown at an angle with a threaded hole in the middle of them. There are six of these surfaces, in pairs, and all of them can be seen in the previous figure. The purpose of these surfaces is to mount clevises that hold the struts to dynamic portion of the BitBox. Toward the bottom there is a 12-bolt-hole circle shown and this is used to mount the bottom portion of the Receiver Assembly to this BitBox Receiver. These components bolt to the underside of the BitBox receiver are used to retain the replacement drill bit assembly in place and

then release it, mechanically, when the robotic arm is in place when to acquire it. The profile of the BitBox receiver somewhat follows the profile of the replacement drill bit assembly and at the same time allows room for the struts to mount to their respective clevis points.

What started as a simple cylinder part that could be easily turned on a lathe to fabricate, ended up as a pretty complex part that could still be turned on a lathe and then also machined with a 5-axis mill. While being more expensive than initially expected, it also incorporated what could have easily been half a dozen components in order to meet all of the design goals, into one part that completed them all. A final touch in order to make the surface have less traction on them when the robotic arm comes in and slides along it, is that this aluminum 7075 part is treated with a Teflon-impregnated hard anodize in order to make this part both as hard as possible and lower the coefficient of friction on it to as low as possible.

2.4.2 ANCILLARY RECEIVER ASSEMBLY PARTS

The section view in Figure 18 shows the complete receiver assembly with a replacement drill bit assembly being retained.

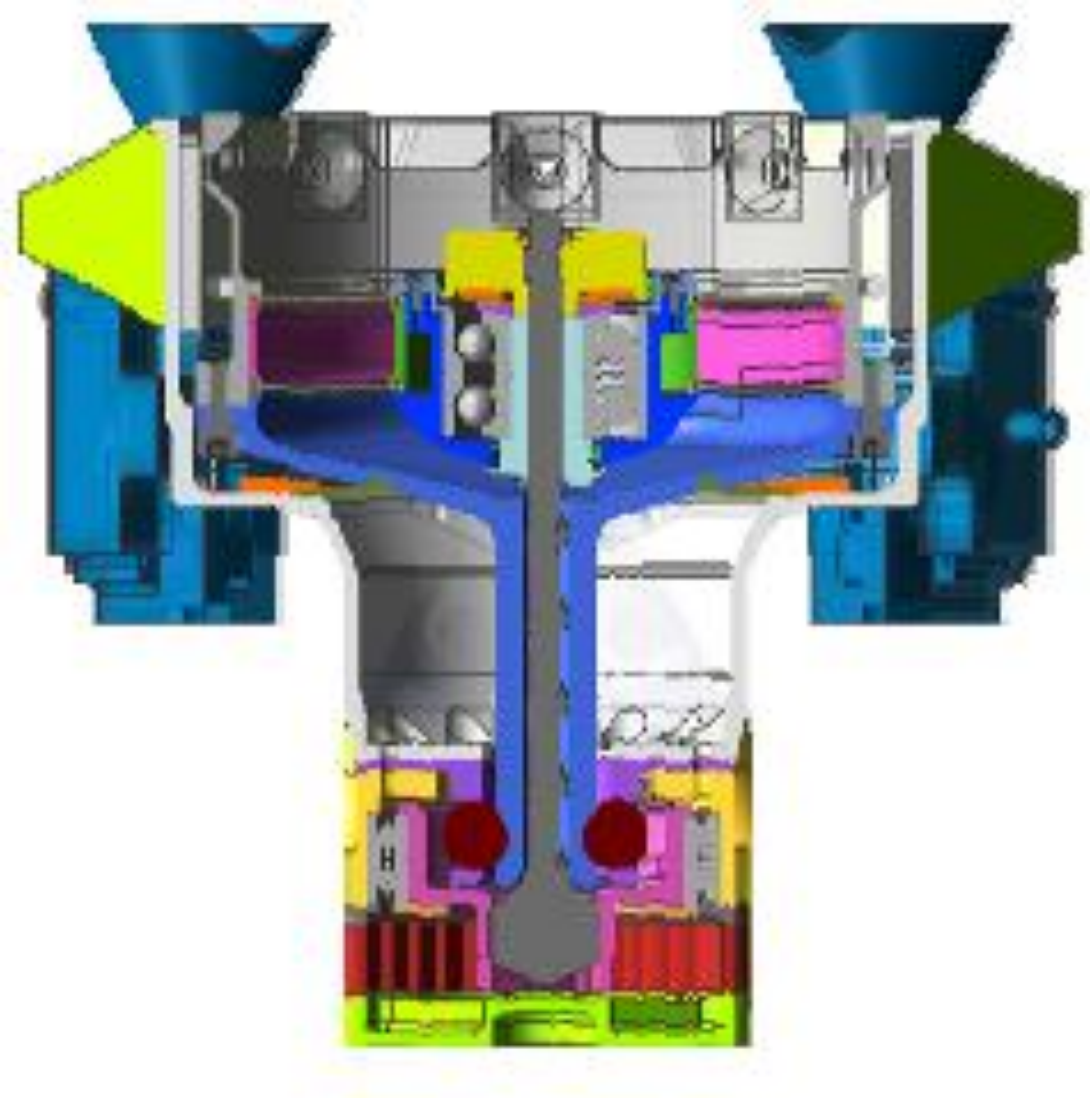

Figure 18 - Receiver Assembly with Drill Bit Assembly, Section View

The purpose of these components is to complement one another in holding the replacement drill bit assembly in place. Figure 19 shows the drill bit assembly being retained within these parts by a ball-detent method.

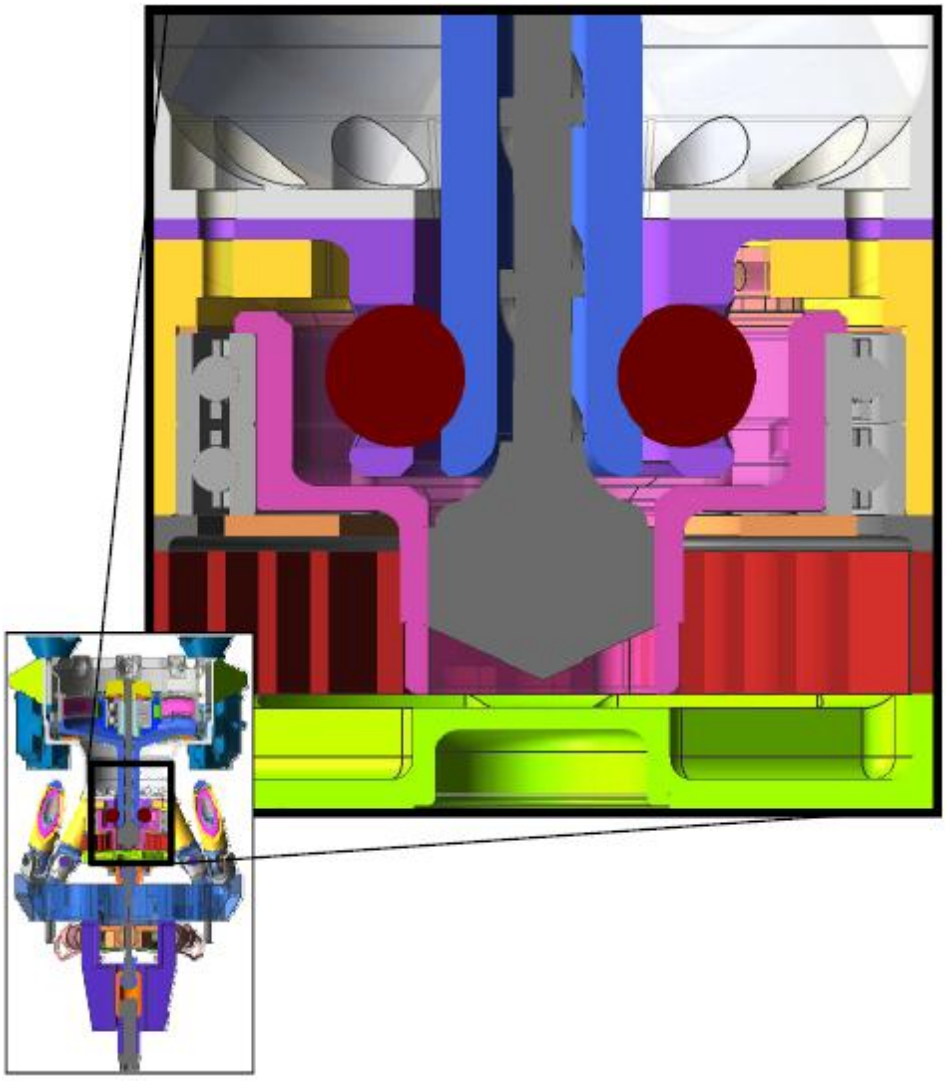

Figure 19 – Ancillary Components, Receiver Assembly

This ball-detent method utilizes a square cam profile in order to manipulate the balls into one of two configurations. The first is to hold the balls in against the drill bit assembly, locking it in place. The second is to allow the balls to move, thereby releasing the drill bit assembly. These configurations are displayed in the top-down section view through the bit retaining balls in Figure 20.

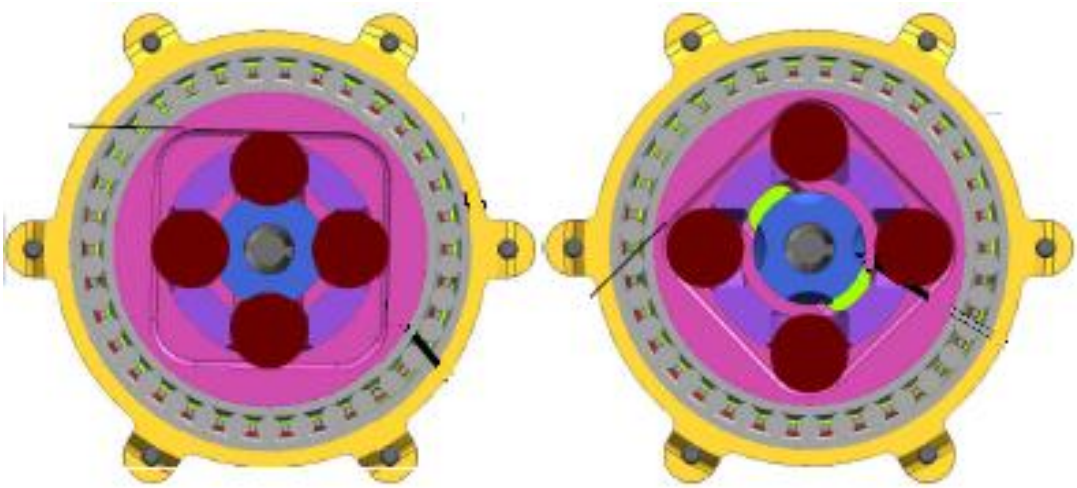

Figure 20 – BitBox Cam, Locked (L) and Unlocked (R)

The picture on the left shows the replacement drill bit assembly being retained. The BitBox cam is shown clamping the Bit Retaining Balls in to the detents. The picture on the right shows the BitBox cam rotated 45 degrees in order to allow the ball to translate radially outward and the drill bit assembly is now free.

There are two bearings on the outer perimeter of the cam that allows a smooth rotation to occur when torqued by the robotic arm. There is also a ball retainer that allows the bit retaining balls to translate outward radially but will always remain in their cavities in this part.

The torque required to release the replacement drill bit assembly is shown in the Graph 1 below.

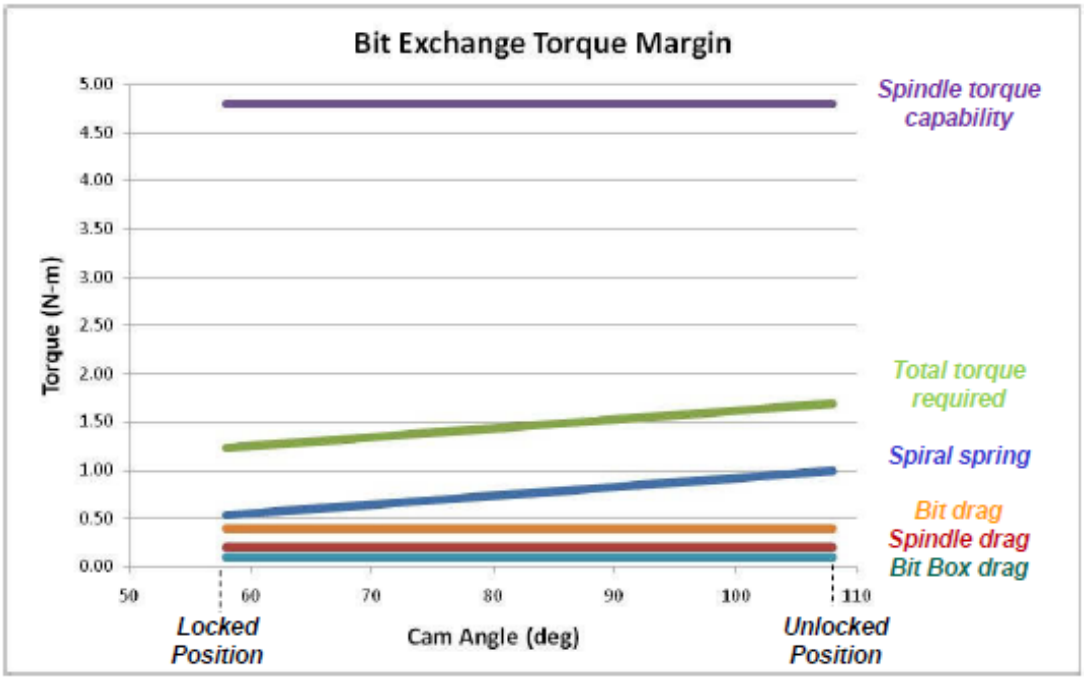

Graph 1 - BitBox Torque Requirement

The total torque required to release the replacement drill bit assembly is shown to have a calculated nominal value of 1.7 N-m. The torque value is created by a combination of various drags in the receiver assembly, due to friction, and most notably from the clock spring preload. At the top of the graph is the spindle torque capability line which is provided by the robotic arm and has a nominal value of 4.8 N-m. As long as the drag values do not exceed the capability value then the robotic arm can acquire the replacement drill bit assembly. In a worst-case scenario, the replacement drill bit assembly can be released with about 1/3rd the torque capability of the robotic arm.

2.5 MICRO-SWITCH ASSEMBLY

The micro-switch assembly is the critical feedback aspect of the BitBox in that it gives the signal to the Rover that the robotic arm has successfully docked with the BitBox. This is done through a combination of electrical and mechanical mechanisms. The robotic arm has sensitive alignment posts that are utilized to act as feelers when it is in place to receive a replacement drill bit assembly. Those alignment posts are used opposite of the BitBoxes' alignment cones. These alignment cones are the first aspect of the micro-switch assembly and are displayed in Figure 21.

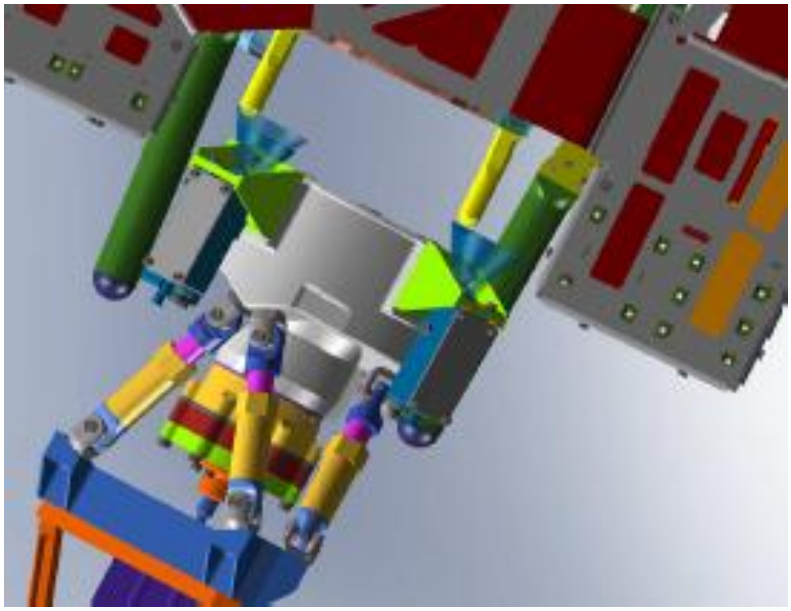

Figure 21 – Robotic Arm Alignment Posts Docking with Micro-Switches

Once the alignment posts are within the in interior conical volume of the alignment cones, then they are guided by the geometry of the cone down toward the micro-switch. Figure 22 shows the full assembly of the micro-switch.

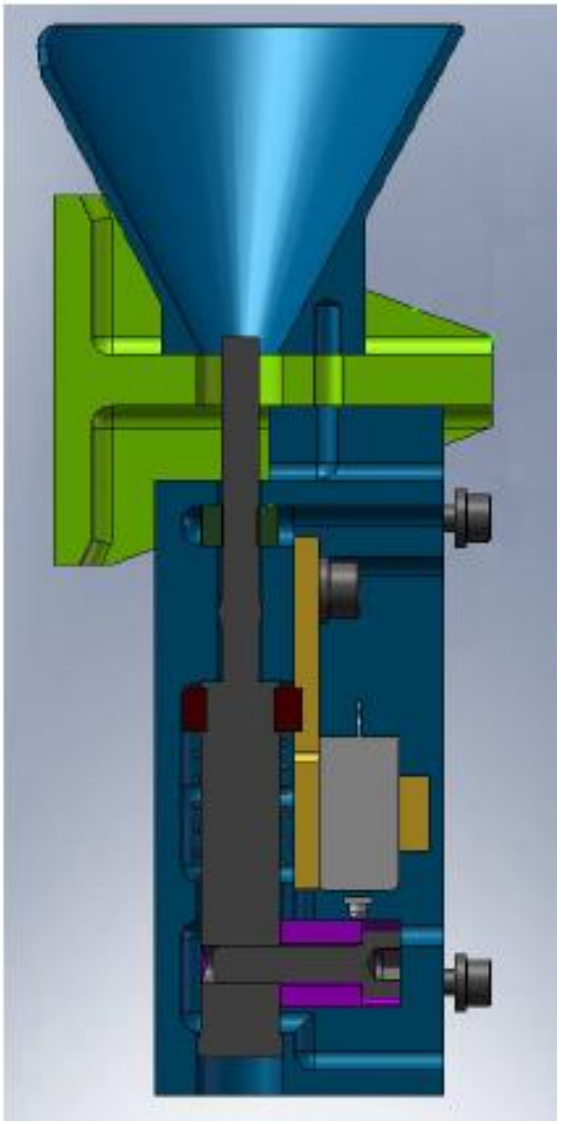

Figure 22 - Micro-Switch, Section View

The alignment cone is at top and mounts to a bracket shown in lime green. This bracket is directly mounted to the receiver assembly in four locations as previously detailed. On the underneath side of the bracket is the actual micro-switch enclosure. The switch itself in made by Honeywell and is shown in grey. It is preloaded to close the circuit and it is therefore the job of the robotic arm alignment posts to engage a plunger that releases the contact with the switch. It is now open and if three of the four micro-switches signal that they are open, the replacement drill bit assembly procedure can commence. This switch box is completely encloses so that no dust or other particulate can interfere with the switch motion. The front and side detail views in Figure 23 give a better representation as to the function of the switch.

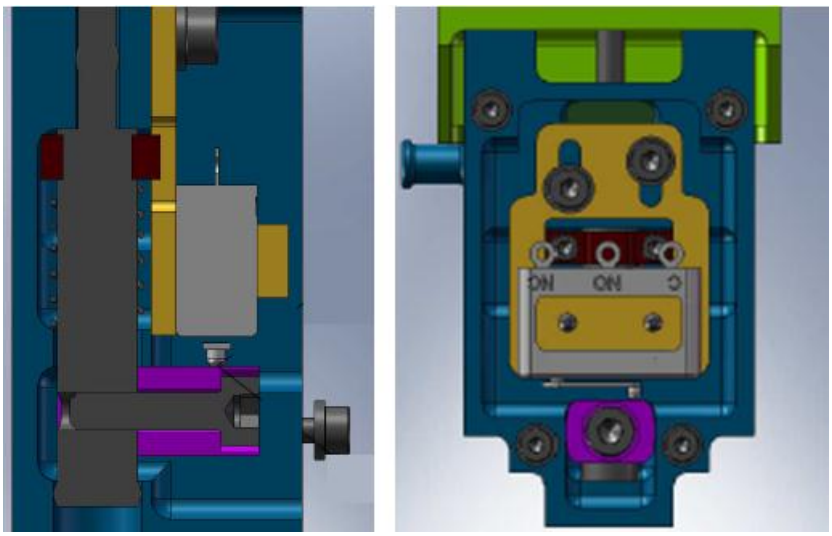

Figure 23 - Micro-Switch Assembly, Side and Front View

As can be seen on the side view, the plunger is also given a preload with a small spring that needs to be compressed in order for the switch to be released. The anvil, shown in purple, is screwed into the plunger and is what contacts the micro-switch. When the plunger is forced downward by the alignment posts, the anvil goes with it. The switch itself is mounted on a separate plate, in yellow, that can be adjusted 2.5mm in order to finely tune each micro-switch assembly. All of these items are mounted or otherwise housed with a two part enclosure. The main part is the structure and is shown in blue, and it gets enclosed by a plate that was omitted from the view to allow the internals to be displayed. As these are the only electrical component on the BitBox (other than the pyro-cutters on the structure) there is also a cable port which allows cables to enter the inside of the micro-switch assembly. This feature can be seen on the front view of the previous figure, on the top-left side of the assembly. As a final aside on the micro-switch assembly, there are four total assemblies on the BitBox. Three of those are identical but die to a close clearance with a portion of the robotic arm, the final micro-switch assembly has a slightly modified alignment cone and bracket, while the housing portion of the assembly is completely identical.

2.6 STRUCTURE

Due to the orientation and accessibility of the robotic arm to the front panel of the Rover where the BitBoxes are to be mounted, neither BitBox was in the same X-Y-Z coordinate system. Further adding to the complexity was that both BitBoxes had different vector orientations and that there were a total of seven inserts on the front panel of the rover in which to mount the two BitBoxes. This implies that one BitBox structure would be mounted to the structure by four bolts while the other would only be in three locations. Therefore, the geometry of these two structures are both complex and unique to the BitBox that they represent.

An initial design concept was to do a riveted and bonded tube structure similar to what had been done to standoff other sub-assemblies both on the rover and in previous missions. However, it was very important to have the plane that the BitBoxes were bolted to on top of these structures to be very precisely located in all 6 degrees of motion. Riveted and bonded structures usually have a lot of assembling time especially where tight tolerances have to be hit. That idea was thereby scrapped as at the time schedule was the driving issue and instead these structures were machined out of solid block of 7050 aluminum alloy. Figure 24 shows the

two structures in their bolt down locations with the structure for BitBox 1 on the left and the structure for BitBox 2 on the right.

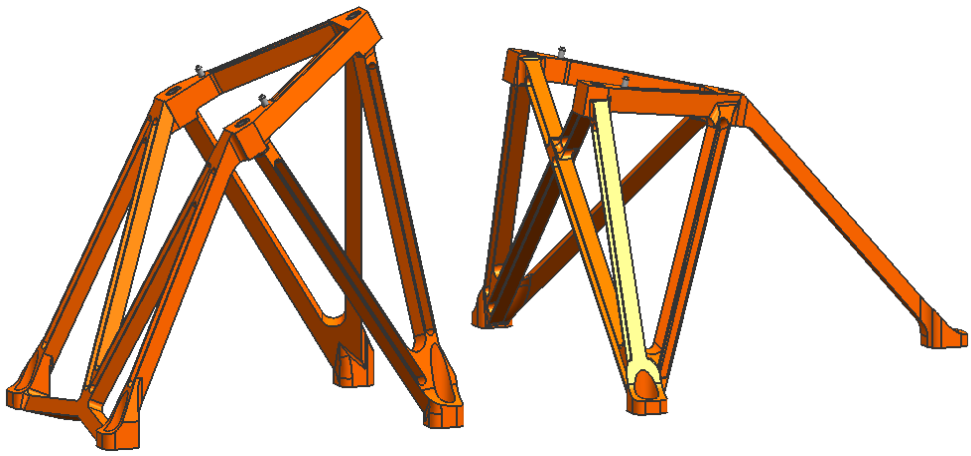

Figure 24 - Structure, BitBox 1 (L) BitBox 2 (R)

Further complicating the issue of these was when a modal frequency analysis was run on these under the launch and landing accelerations and frequencies, there was significant vibration occurring within these structures that translated up to the BitBoxes. The solution was a change in cross-sectional area in all of the legs. What was initially rectangular shaped became an 8mm square shape that was then machined into square C-channel with a 1mm wall thickness for the legs and a 2mm wall thickness for the base. This can also be seen on the legs in the previous figure. While the resulting stress inflicted on the structures increased due

to the change in cross-sectional area, it was still well within factor of safety values. The more important issue was that the frequencies that were seen in the BitBoxes were now gone and the design was approved to be manufactured. These stresses and frequencies will be detailed with FEA plots in Chapter IV.

While the flight models were being machined out of a solid piece of 8 inch thick aluminum, SLA prototypes were also created. The reasoning was such to check and make sure there were no errors hidden in the design, as the geometry of these parts was complex. There could have been some errors within the CAD file data that could have gone unnoticed until the machining was complete. The results are shown in Figure 25 and have a soda can provided for scale.

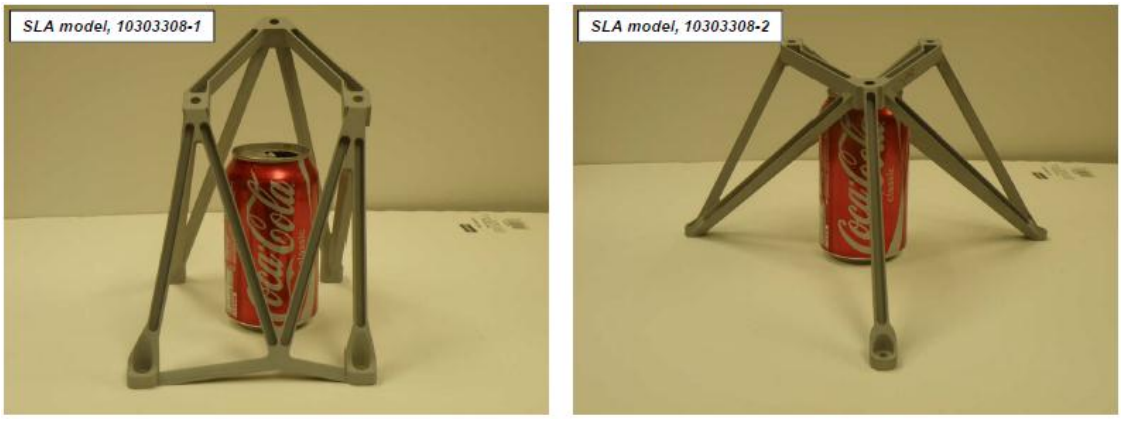

Figure 25 - Structure Prototype, BitBox 1 (L) BitBox 2 (R)

2.7 LAUNCH-LOCK ASSEMBLY

Due to the mobility in the Stewart Platform design of the BitBox, the assembly must be locked in place until it lands on the surface of Mars. There are two ways to accomplish. Either the struts can be fully extended or fully compressed thereby fixing the structure in place and insuring that it will not be able to come loose when it undergoes the significant G-forces of acceleration leaving the Earth and deceleration upon entry onto the Martian atmosphere.

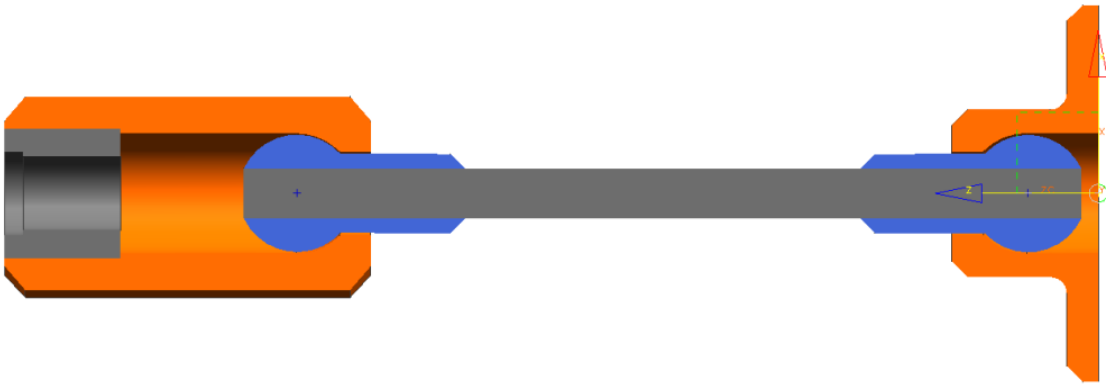

Figure 26 - Launch-Lock Assembly

The best locking direction is to pull the BitBox down such that the springs are in compression opposed to tension. This is accomplished by pulling the moveable portion of the BitBox down toward the front panel of the Rover, and securing it against the fixed portion of the BitBox which is the

base plate of the hexapod. This is done quite simply with a tensioning cable that is shown in the launch-lock assembly in Figure 26.

In order to release this locking feature, a pyro-cutter is to be used.

Figure 27 - Pyro-Cutter, Launch-Lock Assembly

Pyro-cutters are frequently used for single-use space applications. The operation is that the part that is to be cut, in this case a cable, passes through the pyro-cutter which has a blade on one side and an anvil on the other to act as a hard stop, as shown in Figure 27. An electrical signal triggers an explosive charge that directs the bladed through the item to

be cut is a guillotine fashion. Once the cable is severed, the BitBox is released and is now in the deployed configuration. This all occurs long after the rover has landed on the surface of Mars and will actually not be triggered until it is necessary for the robotic arm to acquire a replacement drill bit assembly.

Figure 28 shows the launch lock assembly in the center and toward the bottom. It is tensioned, and as a result compresses the springs, through the use of a single screw at the very bottom. The tensioning portion is housed in a separate bracket that also covers the pyro-cutter. The figure is showed in its tensioned, and thus, launch configuration.

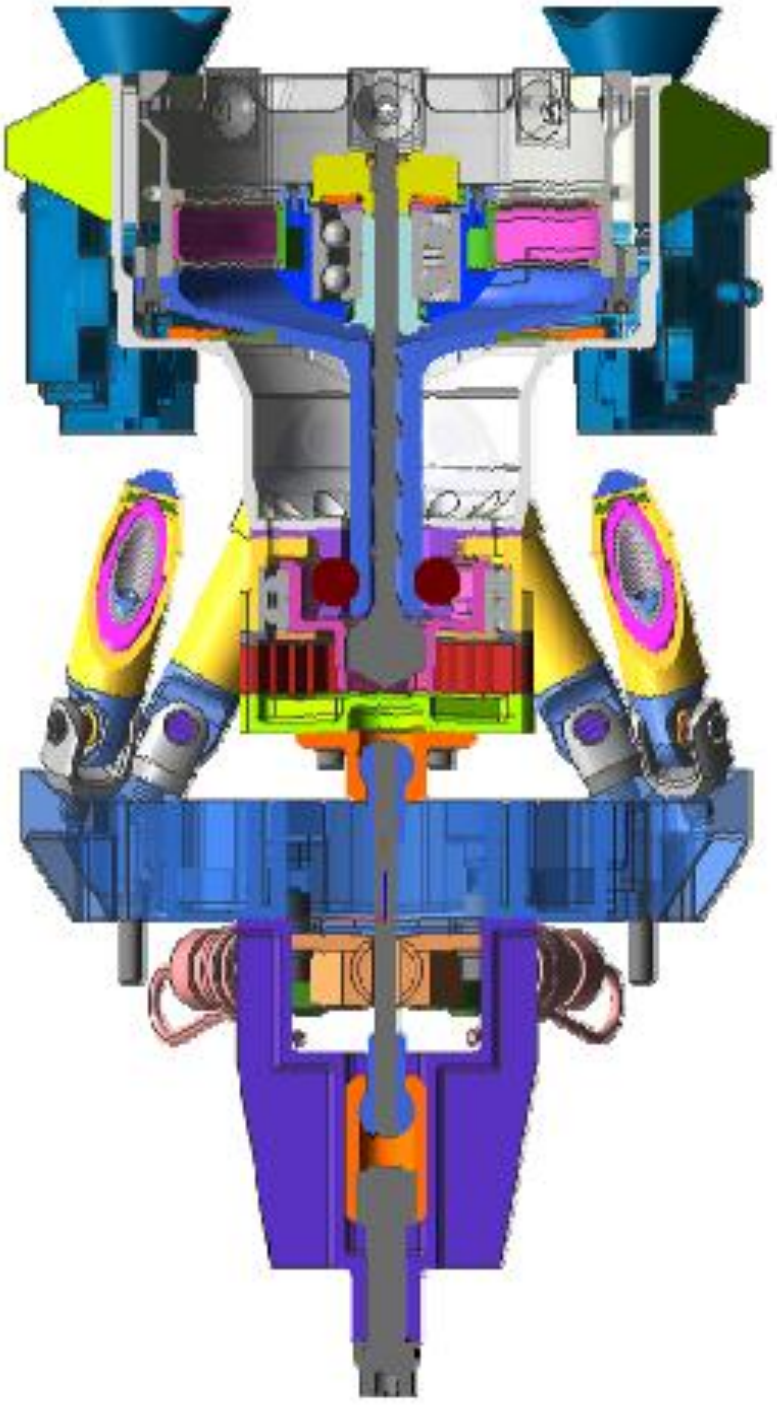

Figure 28 – Tensioned Launch-Lock Assembly, Section View

One final addition that had to be added was an energy absorber. This was because the steel cable is under such tension that when it is cut, the balls on the ends of the cables can cause serious damage to anything in their path. With the majority of the BitBox being aluminum, the steel cable and balls are the stronger material. The solution was to add a thin circular plate that would absorb this release of energy. The idea was that this plate is meant to be sacrificial by the release of this stored energy. However, it must also remain trapped within its enclosure so as to not fall out and interfere with the function of the BitBox. This disc can be seen in Figure 29.

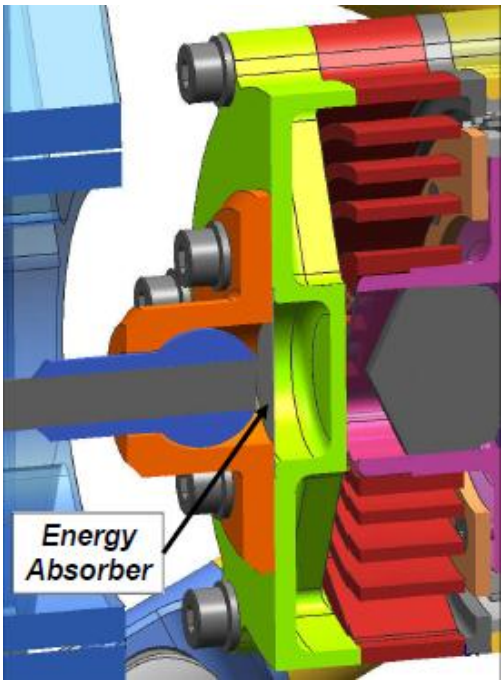

Figure 29 - Energy Absorber, Launch-Lock Assembly

2.8 CABLING

A design goal for the BitBox was to have as few electrical components as possible and to have as much as was feasible be mechanical components. The reasoning behind this was because there was a limited number cable terminals available and if the BitBox design required more than there would be significant design change going back down through the system. Coupling that with the face that this was the last item to be added to Rover, any additional system level changes would have been detrimental to the testing and delivery schedule.

With these considerations in mind, the design was met in that each of the two BitBoxes only required one 10-pin connector, which was all that was available. The items that required cabling were initially just the Micro-Switches, of which there are four per BitBox. Once it was realized that there was a need to lock the BitBox down in place for launch and land, and the pyro-cutters were implemented, an additional cable was required in order to power these. The result was combining eight micro-switch circuits in parallel into four sensing circuits, and two pyro-cuter cable per BitBox. This only accounted for six of the available ten pins per BitBox with the thought that something else might come up during

implementation of the BitBoxes. Luckily after testing the BitBoxes were approved as is and the remaining four pins were just left as open.

With the number of cables decided, the next step was to see the length required in order not to limit the motion of the Stewart Platform. The cables from the micro-switches all needed to run down from the flexible to fixed part of the BitBox. The thinking was that either each micro-switch cable could run down a single strut or they could all be combined prior to reaching the strut and then run down a single strut. The later was what was decided upon to limit the number of service loops and chances for the robotic arm to catch on the cables. This single strut cable run is shown in Figure 30.

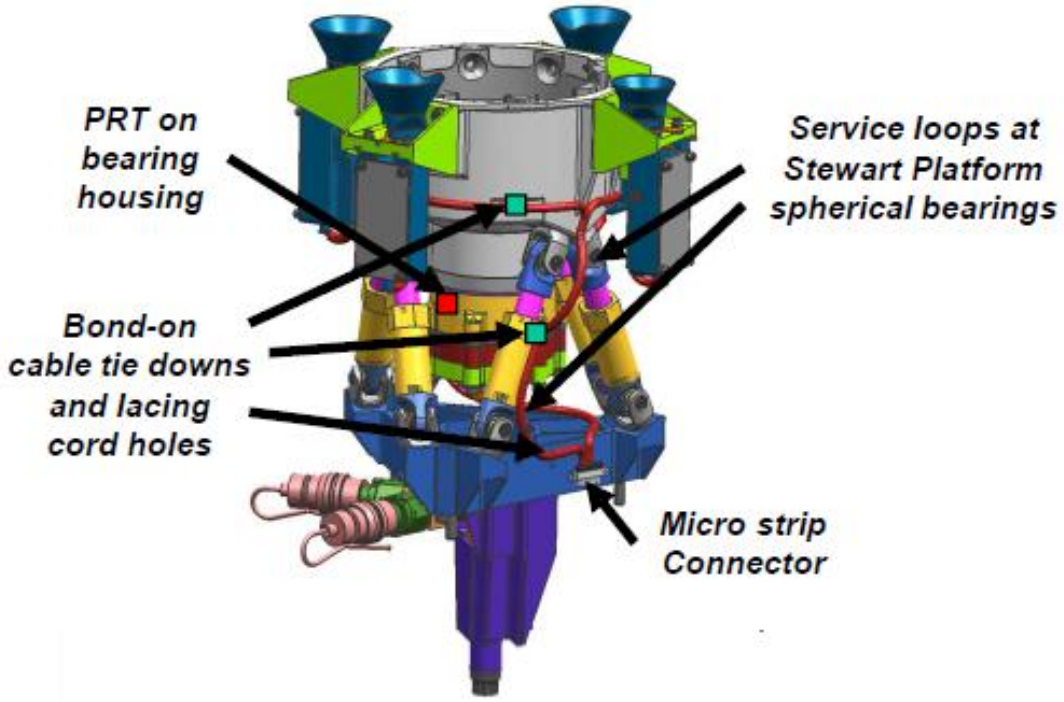

Figure 30 - BitBox Cable Route

In order to limit the motion of cable and to keep them secure against the BitBox, another item that I got to design that was utilized all over the Rover was implemented. This is shown in the previous figure as the bond-on cable tie down. This item is one that I also keep on my keychain as shown in Figure 31.

Figure 31 – Bond-On Cable Tie-Down

This is a very small part that was used in hundreds of locations all over the Rover.

Once the cables reach the baseplate of the BitBox, there is a micro-strip connector that allows the BitBox, as a unit, to be installed and removed as needed. The opposite end of this connector is mounted to the structure that was detailed in Section 2.6. This cable is bonded down to one of the legs of each structure which runs it down to the front panel of the Rover. This is depicted in Figure 32.

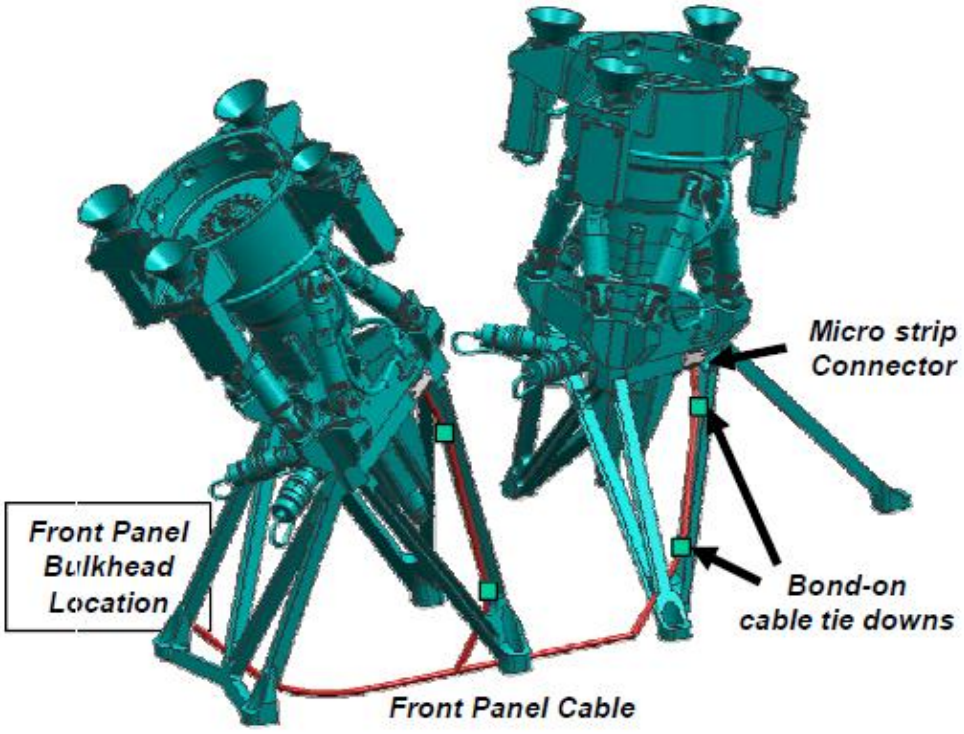

Figure 32 – Cable Route, BitBox to Rover

The pyro-cutter cables also run down the legs of the structure and onto the front panel of the Rover. All the cables then go off to their respective 10-pin connectors that are on the sides of the front panel. The cabling was extensively tested, with complete success, prior to mounting it to the Rover.

This concludes the component design of the BitBox and leads into the stress analysis that was executed to validate the design.

2.9 KINEMATIC ANALYSIS

MatLab was used to determine the kinematic range of motion of the BitBox. This was done in order to ensure that the BitBox design could accommodate the robotic arm misalignment.

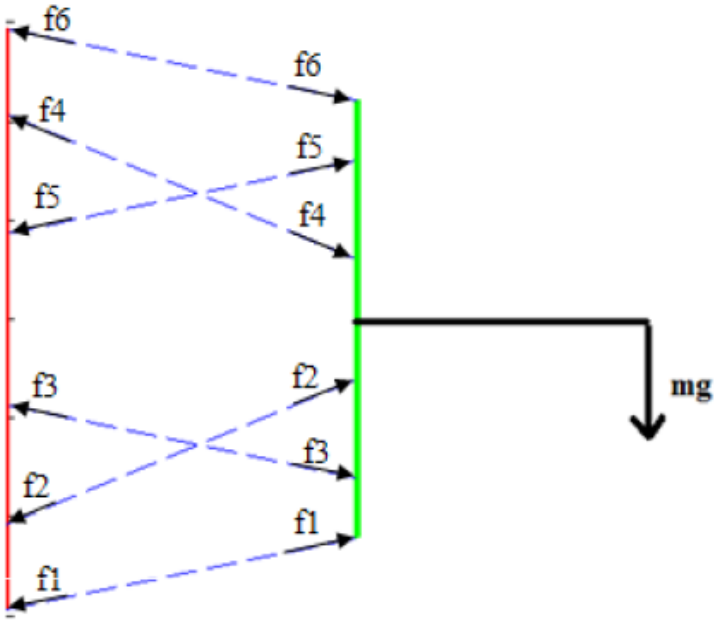

Figure 33 – Kinematic Representation

This is shown in Figure 33 where the left vertical line represents the fixed-plate while the right vertical line represents the free-plate that is allowed to move in the six degrees of freedom. As can also be seen, the gravity vector acts downward placing this Stewart Platform in an undesirable cantilevered position opposed to being strictly in compression or tension.

Also worth noting is that Earth Gravity was used for both testing purposes as well as for figuring in a factor of safety for its operation in the Mars surface where the gravity is only 38% that of here on Earth. This essentially implements a factor of safety of 3 on the design.

The resulting hexapod geometry, obtained through the use of MatLab, dictated the design if the strut length, location, and spring force.

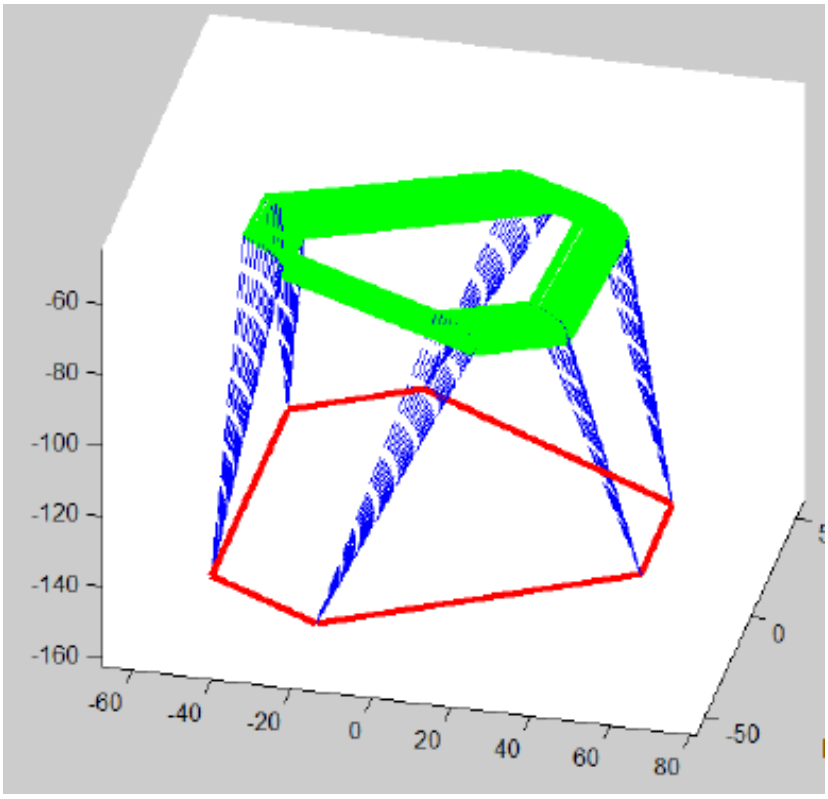

Graph 2 - Free-Plate Range of Motion

Graph 2 shows the finalized plot in MatLab that accommodated the robotic arm error margin of 2 degrees, where the bottom hexagon is the fixed-plate and the top hexagon shows the range of motion of the free-plate. The lines that connect the hexagons by their 6 vertices represent the struts and show the range of motion that has to be accommodated.

CHAPTER III: STRESS ANALYSIS

In order to validate the structural integrity of each of the components, as well as the assembly as a whole, Finite Element Analysis was conducted. This was also used to optimize the weight of the assembly in ensuring that parts were not over-designed and therefore adding unnecessary weight to the MSL Rover. Because the parts were designed in Unigraphics NX CAD, they were analyzed with NASTRAN which is the built in FEA software for this program. The loading that was used is 35 G's (or 35 times the gravitational acceleration on Earth). This encompasses both the worst case launch and landing scenarios. In this chapter the FEA results will be presented and discussed.

3.1 STRUCTURAL REQUIREMENTS

Prior to running any FEA it is essential to know what the requirements are in order to optimize the design. For the BitBox, this includes both the structural integrity of the parts, a thermal check of the BitBox subassembly, and finally a check of the bolted joints to ensure that there was no slippage as a bolted joint is primarily a friction joint.

3.1.1 ACCELERATION REQUIREMENT

The maximum acceleration that the BitBox will experience (as well as the entire MSL Rover) is during the launch operations and landing operations. This value is 35 G's in any direction and includes a factor of safety of two.

3.1.2 CONTACT FORCE REQUIREMENT

The BitBox must also be able to withstand an accidental contact made to any part of it. Within this structural requirement, there were two possible scenarios that needed to be addressed. The first is a 200N inadvertent impact load onto the parts of the structure that are outwardly exposed. An example of this form of load could be from incidental contact with other parts of the Rover during launch or landing. The second scenario is that should the robotic arm not engage the alignment cones properly and instead continues to drive inward on the BitBoxes, the alignment cones need to able to withstand the damage that the robotic arm is capable of creating. The load for this case would be five times greater and a value of 1,000N. Due to this, the alignment cones were fabricated from titanium over aluminum so that they would with stand such a force.

3.1.3 THERMAL REQUIREMENT

The thermal requirement is that the parts need to function during day and night on Mars. The temperatures on the surface of Mars fluctuate much more than on the surface of Earth. This temperature range is from -135°C to +70°C. The BitBox is predominantly made form aluminum, titanium, and steel, so these materials are well within their operational ranges. Parts of similar materials that interface to one another are also not a concern. The issue arises when there is an interface between different materials as the coefficient of thermal expansion varies from one material to another. This can be problematic when one material expands or contracts faster or to a greater degree than another material that has a common interface. When this occurs, either significant stresses can be introduced into the parts or the clamping force on the interfacing surface can degrade causing the parts to slip with respect one another.

3.2 STRUCTURE

The BitBox supports were the cause for the greatest concern from a structural standpoint. Any vibration that the Rover sees during the mission propagates up through the structure of the Rover and cause the BitBox structures to vibrate. Special care was given to analyze these two structures. The material used in both structures is aluminum 7050-T7451 alloy as a significant amount of machining had to be done on these parts (as mentioned in section 3.5).

The two BitBox structures were analyzed in NASTRAN and initially treated as a frame structure. The cross-sectional area of the frame was a square C-channel with dimensions as detailed in Figure 34.

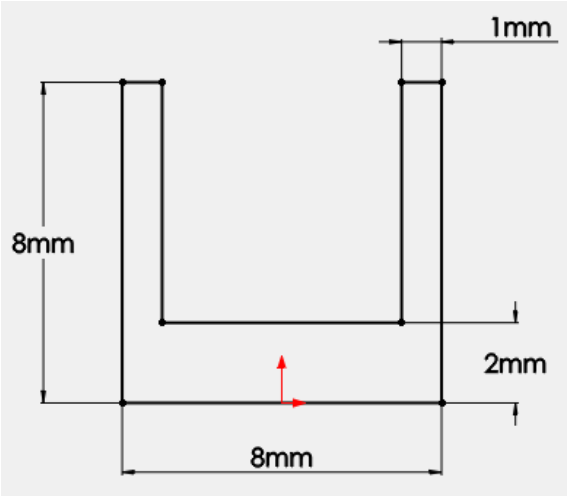

Figure 34 - C-Channel Dimensions, BitBox Structure

However, the interface locations for both the BitBox and MSL Rover were more solid in nature. This was also true for where the various struts came together. Due to that, the parts were re-ran in NASTRAN, this time being treated as 3D solids. The results between the two ended up being similar to each other within 5%. The results plots that are displayed in this section though are the 3D solid versions of the analysis.

3.2.1 BITBOX 1 – STRUCTURAL ANALYSIS

The structure for BitBox 1 utilized four bolts to attach it to the front panel of the Rover and then three bolts to attach the BitBox to this structure. This is shown in Figure 35.

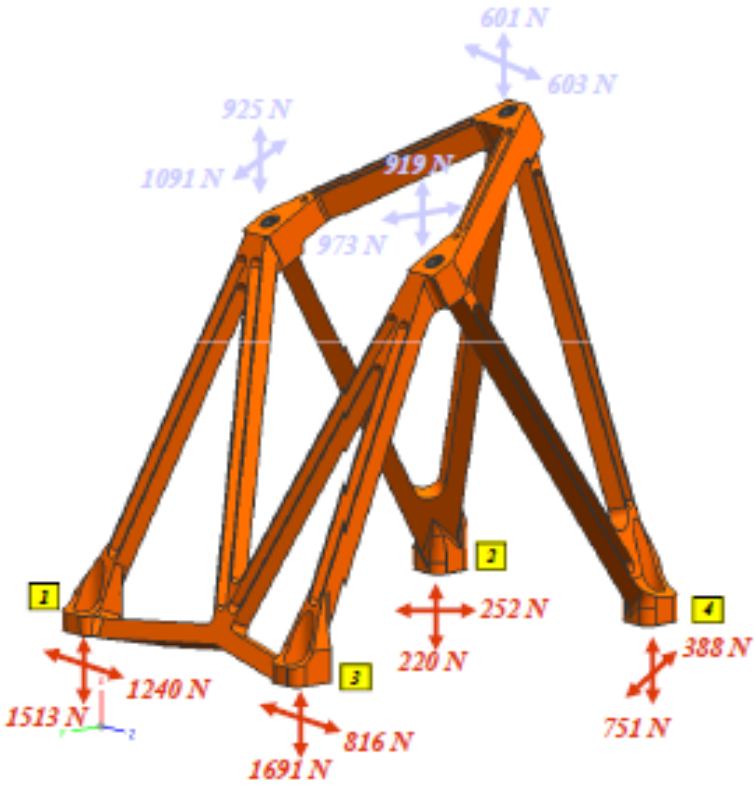

Figure 35 - Constraints for BitBox 1 Structure

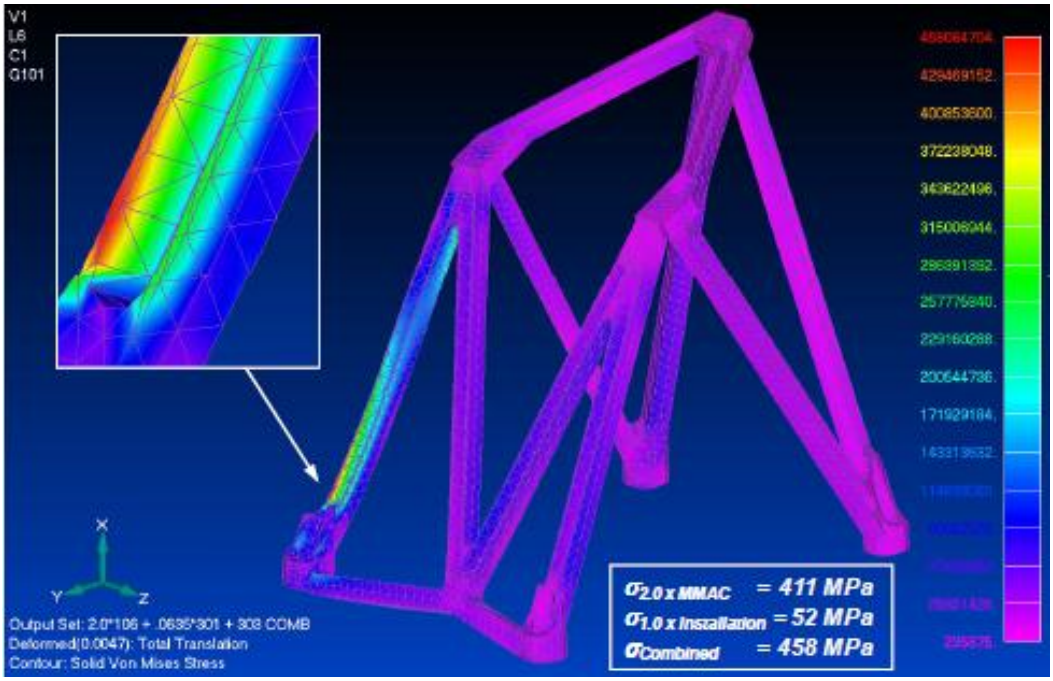

Figure 36 - Stress Plot for BitBox 1 Structure

The maximum stress occurs in the leg as shown in Figure 36. This specific leg had to reach a bolt hole on the MSL Rover that was the furthest away from the center of gravity of the BitBox that it was supporting. The rest of the part is very structurally sound and has very small stress concentrations. However, the stress in the one leg does fall within acceptable values for the loading that it will see so the part is approved.

A modal analysis was performed to determine the fundamental frequency and mode shape. The resulting mode shape can be seen in Figure 37.

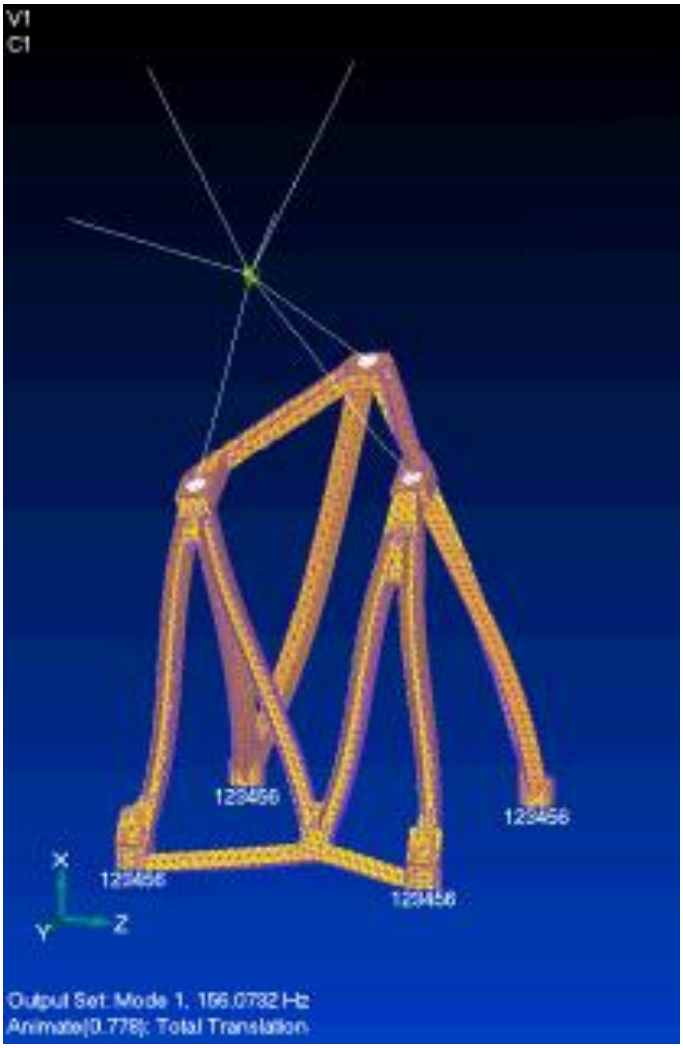

Figure 37 - Mode 1 Shape Plot for BitBox 1 Structure

The fundamental frequency of the part was calculated to be 156 Hz. This is about 2.5 times the requirement of being greater than 60 Hz.

3.2.2 BITBOX 2 – STRUCTURAL ANALYSIS

The structure for BitBox 2 utilized three bolts to attach it to the front panel of the Rover and then three bolts to attach the BitBox to this structure. This is shown in Figure 38.

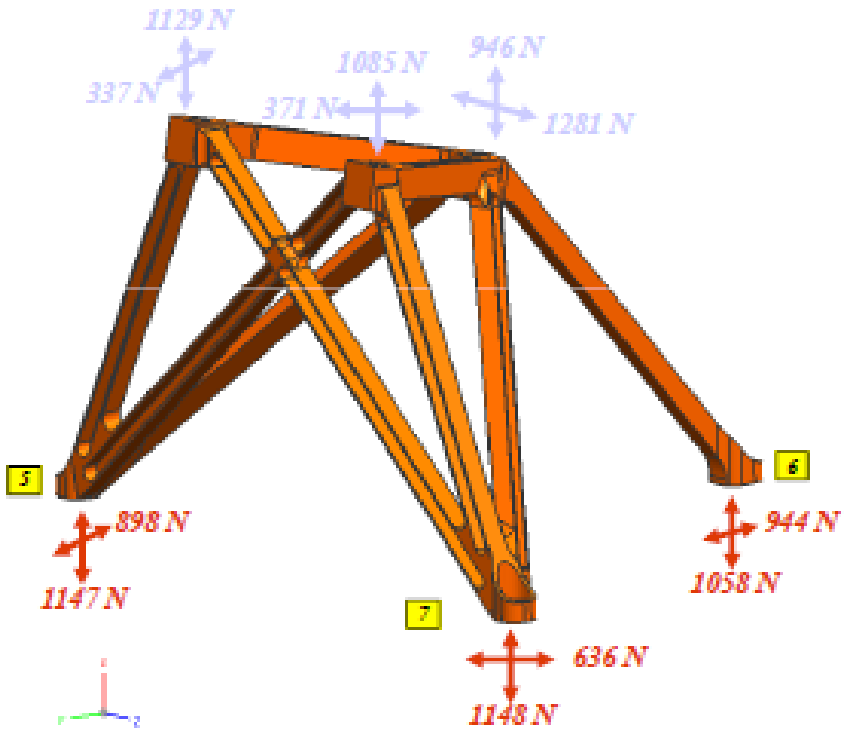

Figure 38 - Constraints for BitBox 2 Structure

The structure was then analyzed in NASTRAN and produced the following stress plot in Figure 39.

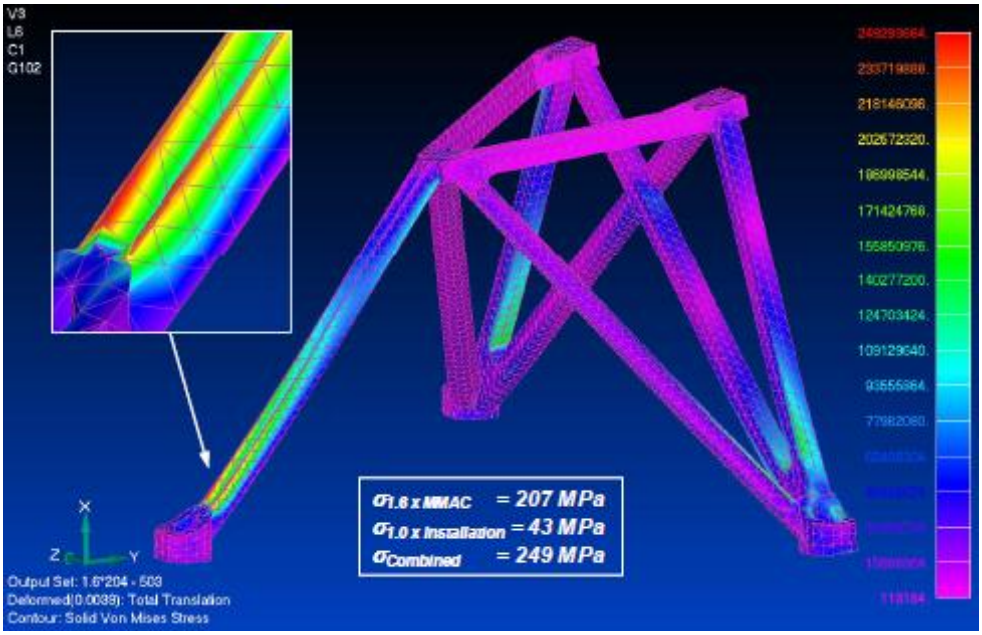

Figure 39 - Stress Plot for BitBox 2 Structure

This symmetry of this part created a more direct path for the stresses to go from BitBox to Rover, when compared to BitBox 1 structure. The result of this symmetry is a stress plot that is more evenly distributed between the three rover panel bolt-hole locations. The largest concentration occurred on the center leg that was both the longest and consisted of only one strut, whereas the left and right legs get the combined stiffness of three struts coming together and therefore better distribute the loads between them. Again the part was within acceptable values of stress, with an included factor of safety value of two, so this part passed as well.

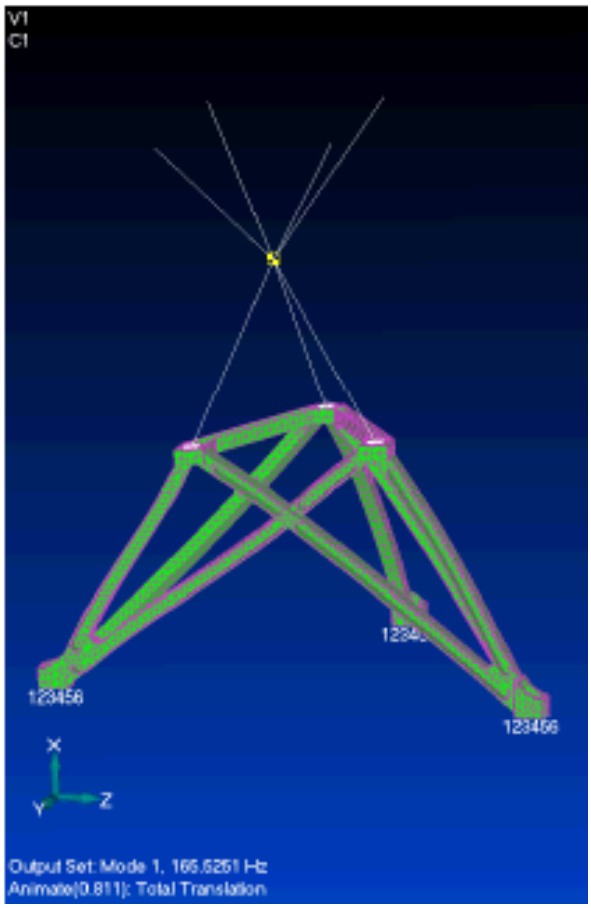

Figure 40 - Mode 1 Shape Plot for BitBox 2 Structure

As shown in Figure 40, the fundamental frequency of the part was calculated to be 166 Hz which is about 2.5 times the requirement of greater than 60 Hz. It is also very similar to the fundamental frequency of the BitBox 1 Structure.

After analyzing the two BitBox structures, the rest of the BitBox parts also need to be analyzed.

3.3 FEA – COMPONENTS

All of the components that make up the BitBox structures had to be analyzed as well. The majority of the changes that needed to be made were simple wall thickness adjustments or rib additions. The following figures in this section are von Mises stress plots for selected parts in the assembly. The material used for these parts is aluminum 7075-T7351 except for the alignment cones (section 3.3.9) which are fabricated out of titanium (Ti-6Al-4V). The yield strength of these materials is 407 MPa for the aluminum parts and 1,000 MPa for the titanium parts. The standard Factor of safety used is 2.0 so all maximum values calculated from NASTRAN must be less than 203.5 MPa for the aluminum parts and less than 500 MPa for the titanium parts. All of the figures show the final stress calculations after all changes had been implemented from previous stress FEA iterations.

3.3.1 FEA – BITBOX RECEIVER

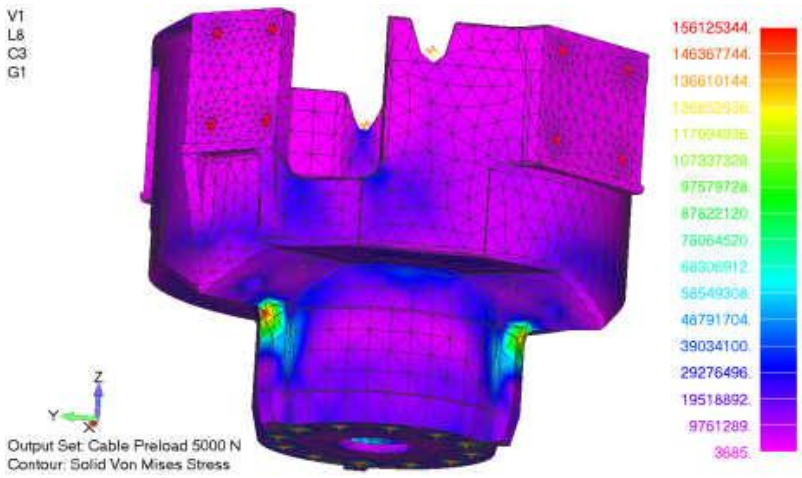

Figure 41 - von Mises Stress Plot of BitBox Receiver

Figure 41 shows the BitBox Receiver with the stress concentrations occurring at the corner where the clevis mount surface comes together with the main cylinder of the part. This could be alleviated with a more generous radius but the calculated maximum stress of 156.1 MPa is well under the 203.5 MPa requirement. It is also of note that the majority of the part is in the purple-blue range which is far less than the requirement.

3.3.2 FEA – BASEPLATE

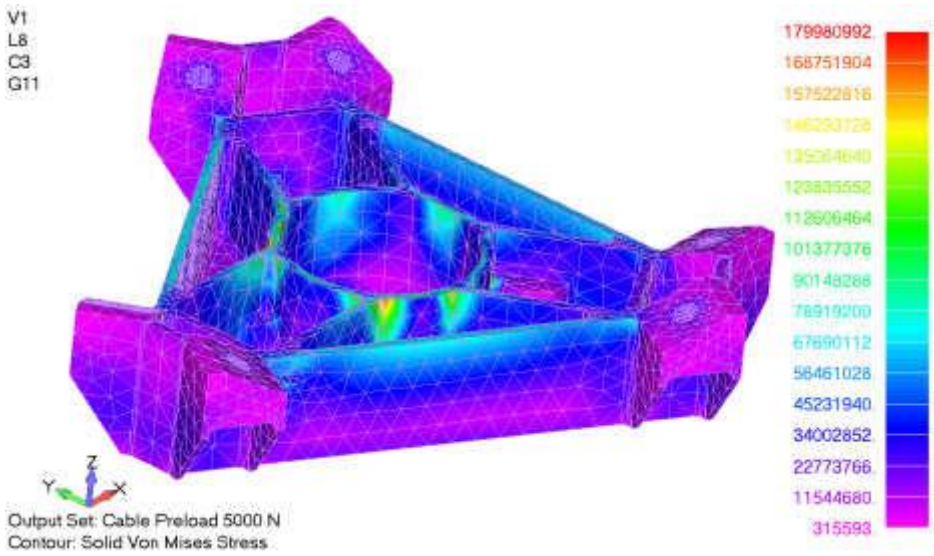

Figure 42 - von Mises Stress Plot of Baseplate

Figure 42 shows the baseplate of the Stewart Platform and has its maximum stress occurring where the internal ribs come together with the center cylinder that allows the cable of the launch-lock cable to pass through. This is to be expected as these ribs were added to the model specifically to carry the load throughout the part and relieve the top surface as it was failing in preliminary FEA iterations. The maximum stress value is found to be 180.0 MPa which is under the 203.5 MPa requirement.

3.3.3 FEA – BOTTOM COVER

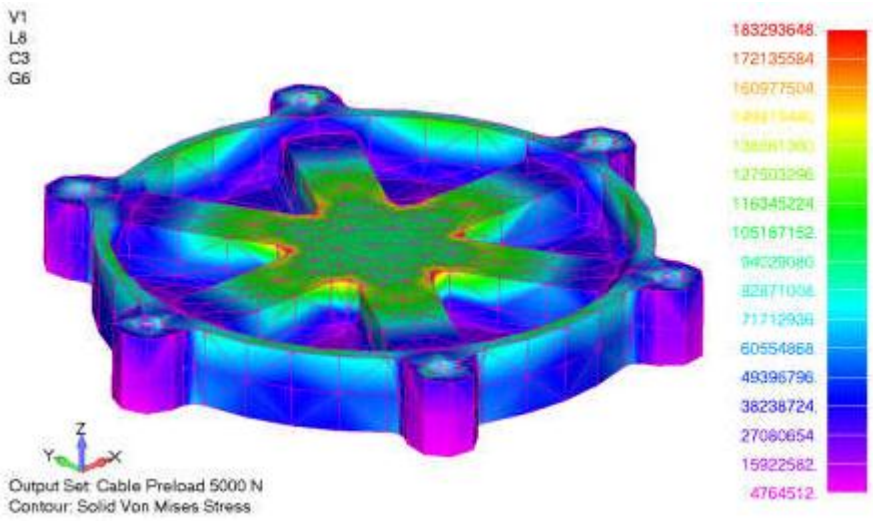

Figure 43- von Mises Stress Plot of Bottom Cover

Similar to the previous part, the Bottom Cover has its maximum stresses occurring where its ribbings come together. This part sees a significant amount of applied load as the launch-lock cable is mounted to the opposite surface to what is shown. Due to this reason, the ribs had to increase significantly in thickness it order to handle this loading and to drive the load outward to the radial mount holes that attach it to the BitBox. The 183.3 MPa maximum stress value is under the 203.5 MPa requirement so this part does pass but did take a significant amount of material increase to the ribs in order to accomplish this. This is all depicted in Figure 43.

3.3.4 FEA – LAUNCH-LOCK BRACKET

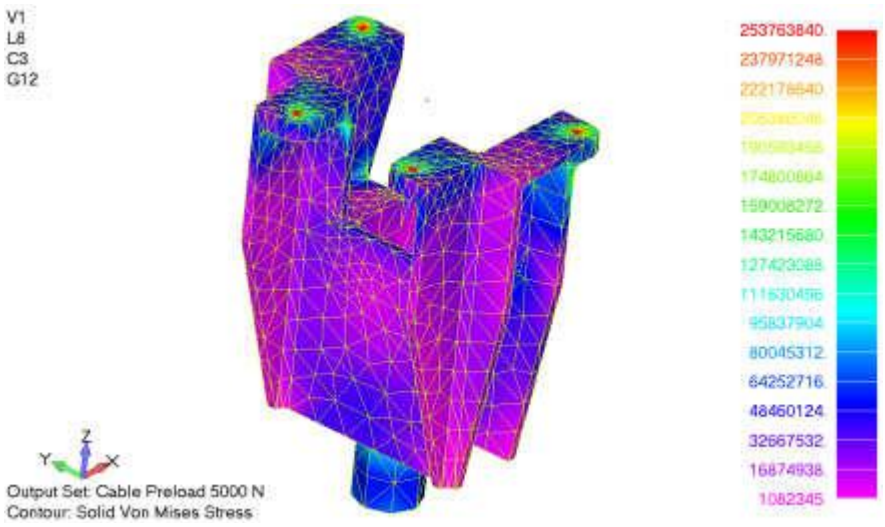

Figure 44- von Mises Stress Plot of Launch-Lock Bracket

Figure 44 shows the Launch-Lock Bracket which, similar to the last part, is responsible for mounting the Launch-Lock Cable and by doing so sees significant amount of loading. This part required a significant amount of ribs in order to drive the load from the cylinder the tensions the cable (at the bottom of the figure) to the four bolt holes that attach it to the Baseplate. As can be seen in the figure, the maximum stress value is 253.8 MPa which exceeds the 203.5 MPa requirement. However, this stress location occurs at the clearance holes for the bolts and when this is the case a one element rule goes into effect. This is basically due to the way that the part is bolted to the structure with a washer that distributes the

load better over the surface at the top and bottom of the hole. What is really happening in this FEA calculation is the by fixing the interior surfaces of the holes this would be more representative of if the part was being pulled in shear against the bolts. The one-element rule is a way to account for the clamping force of the bolt and washer. With that the stress concentration one element away is in the bright green range which represents 174.8 MPa which does get this part approved from a structural standpoint.

3.3.5 FEA – BEARING HOUSING

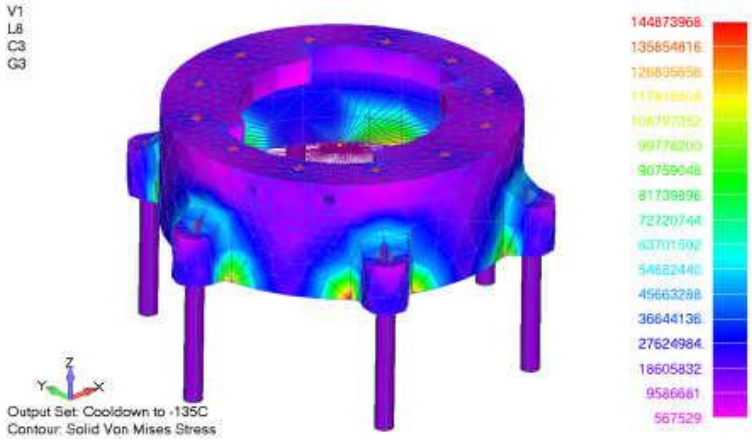

Figure 45 - von Mises Stress Plot of Bearing Housing

Figure 45 shows the stress concentrations of the Bearing Housing. The 6 posts around the perimeter represent the bolts that hold the entire BitBox Receiver assembly together. These are the same bolts that start at the bottom cover, go through various other components and end up in tapped holes in this part. Because the bottom cover sees such a loading from the Launch-Lock assembly, the bolts are pulling down against the six threaded holes to which they are mounted on this Bearing Housing. This accounts for the stress concentration being the highest right where these threaded holes meet the cylinder of the part. However, the 144.9 MPa maximum stress is far less than the 203.5 MPa requirement so this part is approved.

3.3.6 FEA – BEARING CLAMP

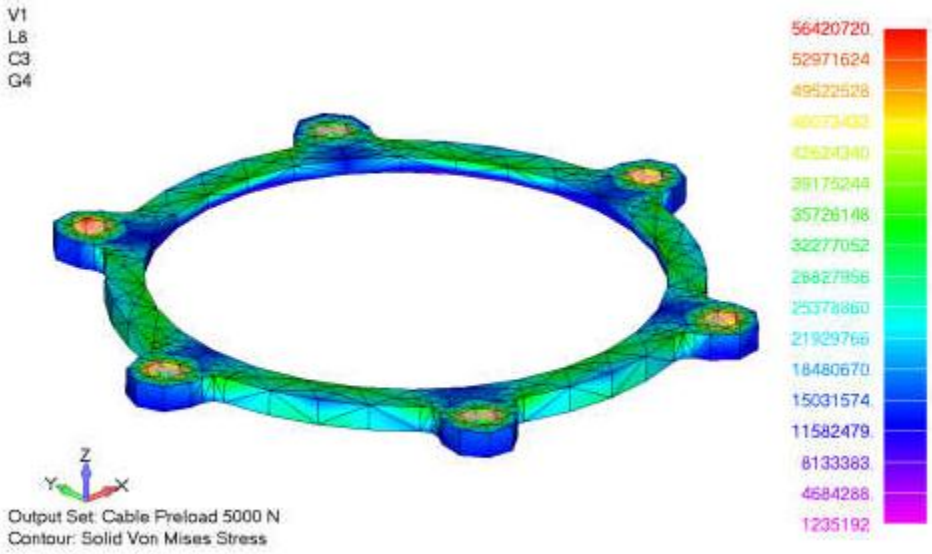

Figure 46 - von Mises Stress Plot of Bearing Clamp

Figure 46 shows the stress concentration for the Bearing Clamp. This part is directly below the Bearing Housing in the previous figure and has the same bolts shown pass straight though its six holes. Because this part is more of a clamp with no direct loading being applied to its holes, its maximum stress value is only 56.4 MPa which occurs at the holes so by using the one-element rule the stress would be more in the 39.2 MPa range (bright green). However, both values are so far under the 203.5 MPa that it passes with or without using this rule.

3.3.7 FEA – BALL RETAINER

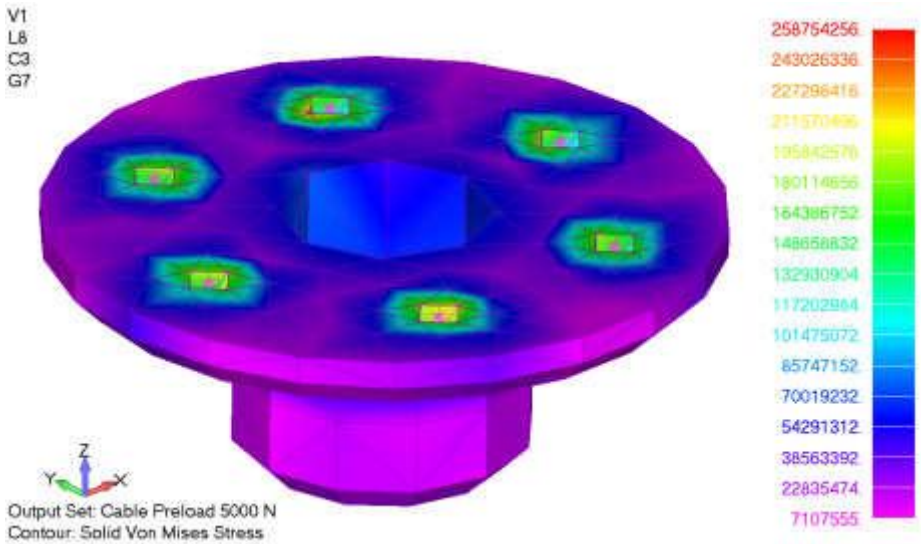

Figure 47 - von Mises Stress Plot of Ball Retainer

Figure 47 for the Ball Retainer of the BitBox, the maximum stress concentrations occur at the bolt surfaces which are fixed in this FEA. Due to this the one-element rule is to be used again brings the max stress down from a failing 258.8 MPa down to a passing 117.2 MPa (teal colored range).

3.3.8 FEA – BALL SHANK HOUSING

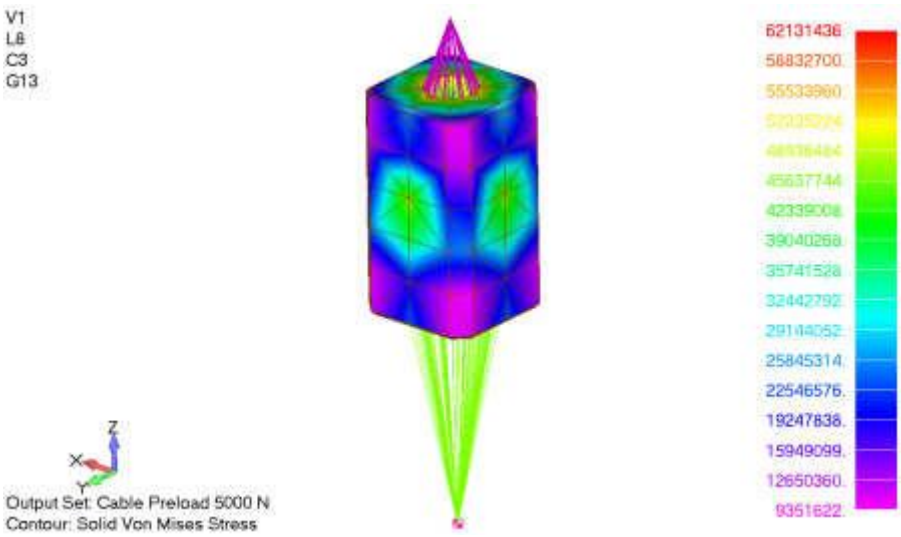

Figure 48- von Mises Stress Plot of Ball Shank Housing

Figure 48 represents the Ball Shank Housing for the Launch-Lock assembly. My anticipation for this part is that it would see stresses exceeding the 203.5 MPa limit but because it holds the Ball Shank around a hemisphere of the ball, this acts as a great form of stress distribution. The 62.1 MPa value is much less than required and while the part could have been modified to save a few grams, the part this fits into, the Launch-Lock Bracket was already in fabrication.

3.3.9 FEA – ALIGNMENT CONES

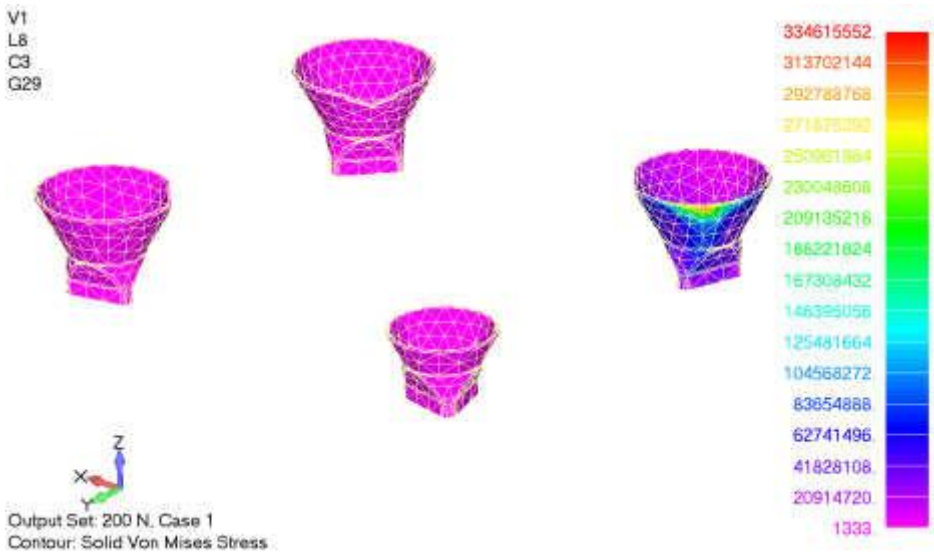

Figure 49- von Mises Stress Plot of Alignment Cones

Figure 49 shows the stress concentration of the Alignment Cones. Due to the symmetry of the part, all four cones were analyzed at one. It should be noted that three of the fours cones are exactly identical but the cone in the bottom position is slightly smaller than the other three. Due to this the larger cones would be analyzed as the compactness of the smaller cones is a better load path. These parts had to be changed from aluminum to titanium as a result of the FEA analysis. The figure represents if the alignment posts of the robotic arm make contact with the edge of the cone and does not go through the proper aligning process. This form

of loading can be quite damaging as the robotic arm would continue translating inward without realization that it was not functioning as intended. This maximum stress value was found to be 334.6 MPa and is less than the titanium requirement of 500.0 MPa. Without making the change to titanium, the FEA could not approve the part without jeopardizing the function of the part.

3.3.10 FEA – ALIGNMENT CONE BRACKETS

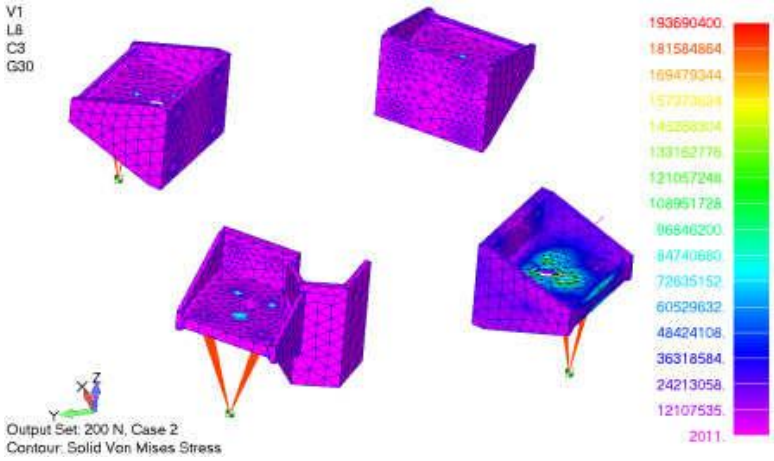

Figure 50- von Mises Stress Plot of Alignment Cone Brackets

This final FEA in Figure 50 for the components section shows the Alignment Cone Brackets to which the previously analyzed Alignment Cones mount to. These parts are aluminum and again have the maximum stress occurring at the bolt holes to a value of 193.7 MPa. While this passes as is, the one-element rule further ensures its success as the value would be more in the 133.2 MPa range (bright green).

Now that the individual parts of the BitBox have been analyzed and approved from a structural standpoint in NASTRAN, a final check of analyzing the complete BitBox assembly will detailed in the next section.

3.4 FEA – ASSEMBLY

After completion of finite element analysis on the individual parts, the BitBox as an assembly was subjected to FEA analysis. It was used with the MSL rover body to which it is affixed as its grounded location. Figure 51 shows where the BitBoxes are mounted and then the corresponding three points to where the MSL Rover body is constrained to its mobility sub-system.

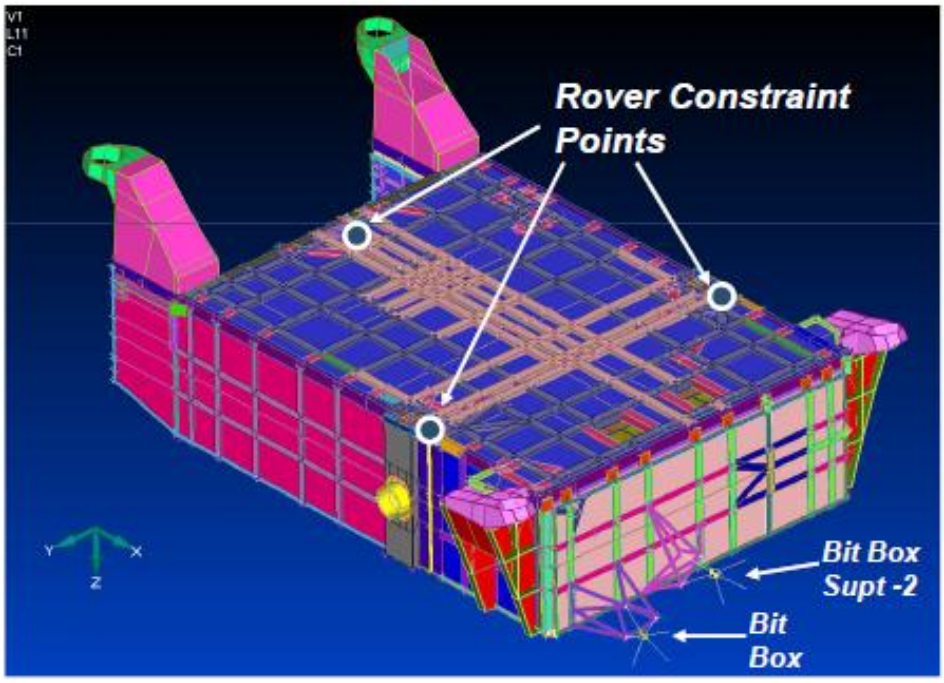

Figure 51 - FEA, MSL Rover Body

With those moment arms applied from the fixed locations to the BitBox mount locations, a mesh was then generated of the BitBox assembly as a whole. The result is shown in Figure 52. The total mass of the BitBox is 2.59 kg and there were 176,000 nodes that were created by NASTRAN to which this assembly was analyzed.

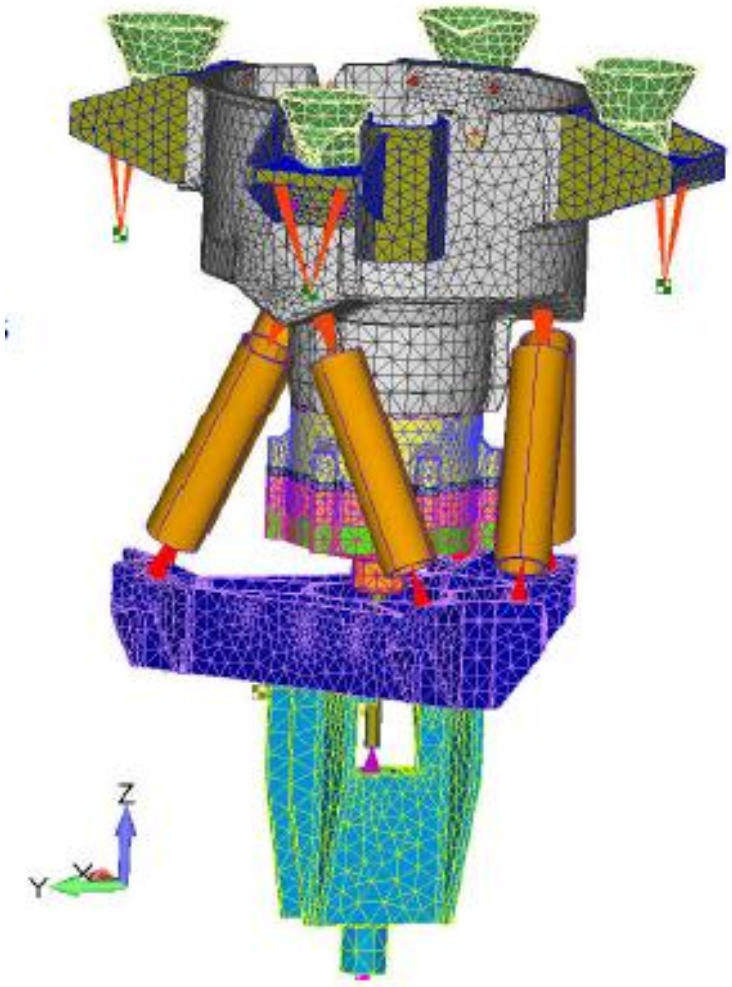

Figure 52 - FEA, BitBox Assembly

There were no surprised in running an FEA of the complete BitBox Assembly. All parts were well within range of yield stresses with a 2.0 factor of safety value applied. All parts also had a first mode natural frequency greater than 90 Hz except for the Clock Spring. However, the Clock Spring so constrained within the BitBox that this mode is dampened out by the rest of the BitBox prior to getting to either the Struts or the Structure which are the parts of greatest concern for the natural frequency.

3.5 BOLTED JOINTS

The final FEA subsection relates to the joints between the parts that are held together by bolts. The biggest issue with bolted joints is torqueing them down to a range that adequately clamps the part while not over torqueing the bolts which could damage the threads that are in aluminum parts. These calculations were done utilizing a table created by another engineer who has 20 years of experience in dealing with bolted joints. In using this table, Table 1 below, some of the bolt sizes and tapped holes that I had placed in the model needed to be increased to eliminate the possibility of slipping of the bolts.

Table 1 - Bolted Joints - BitBox

Interface	Bolt size	Bolt no.	Ultimate Strength (N)	Yield Strength (N)	Nominal Preload (N)	Thermal Preload gain (N)	Thermal Preload loss (N)	Critical Load Condition	Max Shear (N)	Max Axial (N)	MS ultimate	MS yield	MS slip	MS gapping	MS bolt shear
Cone / Cone Bracket	MJ2.5, 1250MPa	4 x 3	4600	3870	2300	90	-279	1000N on 1 cone	461	1997	0.16	0.01	-0.23	0.24	4.70
Cone Bracket / Receiver	MJ3, 1250MPa	4 x 4	6800	5710	4280*	216	-669	1000N on 1 cone	1017	1088	0.17	0.00	-0.48	3.03	2.72
Receiver / Outer Bearing Housing	MJ2.5	12	4050	3045	2030	192	-62	Cable Preload	168	524	0.40	0.08	0.43	2.98	
Outer Bearing Housing / Bottom Cover	MJ3	6	5980	4500	2990	25	-78	Cable Preload	19.8	387	3.40	1.03	21.6	4.75	
Bottom Cover / Ball Shank Mount	MJ3	6	5980	4500	2990	11	-4	Cable Preload	1495	1015	0.49	0.14	N/A	1.87	
Base Plate / Structure	MJ5, 1250MPa	3	19100	16100	12000*	734	-2276	MMAC	1281	1129	0.23	0.05	0.01	8.63	
Cable Cutter / Base Plate	MJ5	2	16800	12700	8410	734	-2276	Launcb, 35g	35.5	201.1	High	High	High	High	
Tensionier / Base Plate	MJ3	4	5980	4500	2800*	264	-819	Cable Preload	1040	1582	0.29	0.01	N/A	0.32	
Tensionier	MJ8	1	45900	34500	22900	734	-2276	Cable Preload	small	5000	High	High	High	High	

** These preload values are not standard*

The conclusion for this is that after resizing several of the bolted joints, all are within margins of safety for their respective joint responsibility.

CHAPTER IV: OPERATION

4.1 INTERFACE

The BitBox acts as the interface between the body of the Rover and the robotic arm of the Rover. The robotic arm is mounted to the front panel of the Rover, which is also where the BitBoxes are mounted. This is shown in Figure 53 as a CAD model.

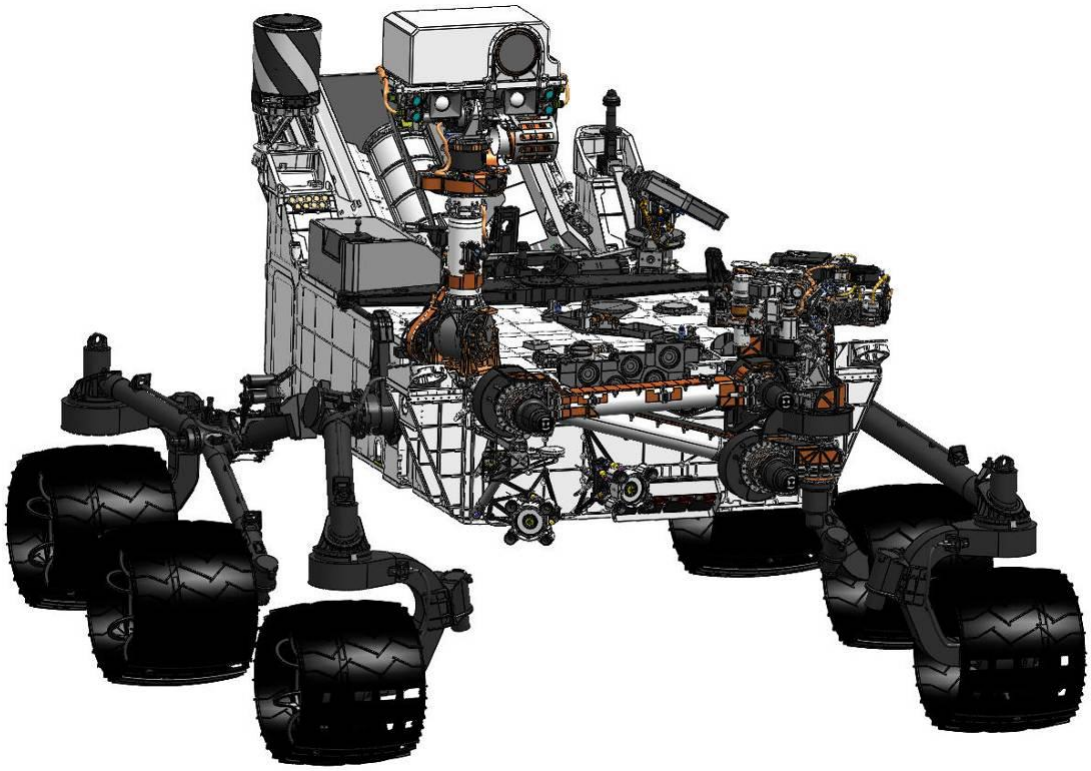

Figure 53 - MSL Rover Front Panel

Three interfaces must be considered. The first is a fixed interface on the front panel of the Rover body and the mounting structure of the BitBoxes. The second is the replacement drill bit assembly and the robotic arm. The third is a compliant interface that absorbs and directs the robotic arm. This one is between the drill bit assembly and the BitBoxes.

4.1.1 INTERFACE 1 – ROVER BODY TO BITBOX

Due to the BitBoxes being a late addition to the Rover, there were no set mount points which we were able to define. Instead, the front panel of the Rover was designed with extra mount points in case items were to be added. There were a total of seven of these mount points that were able to be efficiently accessed between the two BitBoxes; Four by the outboard BitBox and three by the inboard BitBox. The location of the two BitBoxes can be seen in Figure 54.

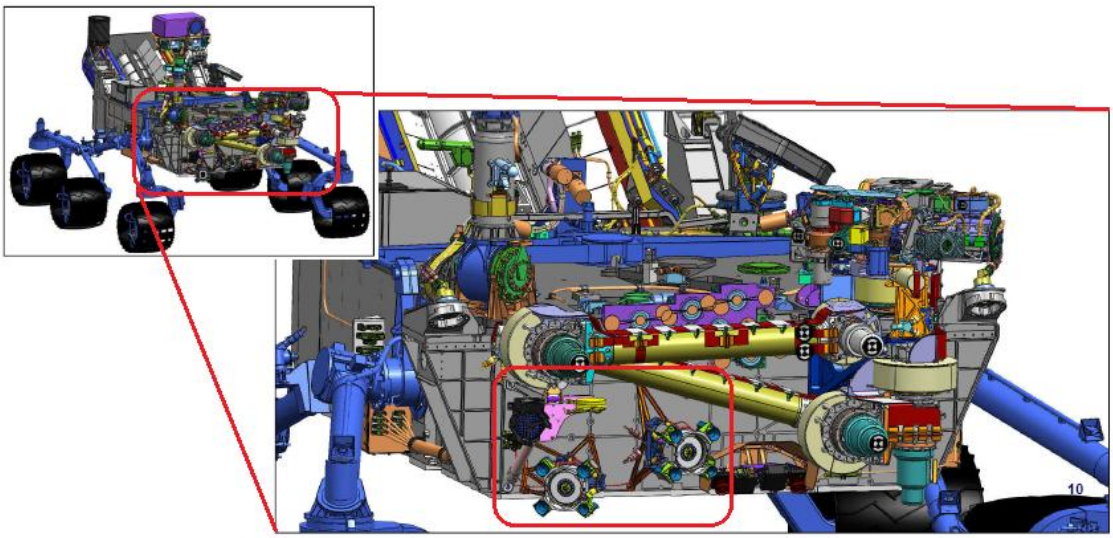

Figure 54 – Interface, Rover Body to BitBox

4.1.2 INTERFACE 2 – BITBOX TO DRILL BIT ASSEMBLY

The BitBox had to be designed to work with the existing drill bit assembly. However, there were existing detents in the drill shaft housing for drill bit assembly removal during testing that we utilized as the interface for the BitBoxes as well.

Figure 55 shows the detents at the base of the shaft near the drill bit.

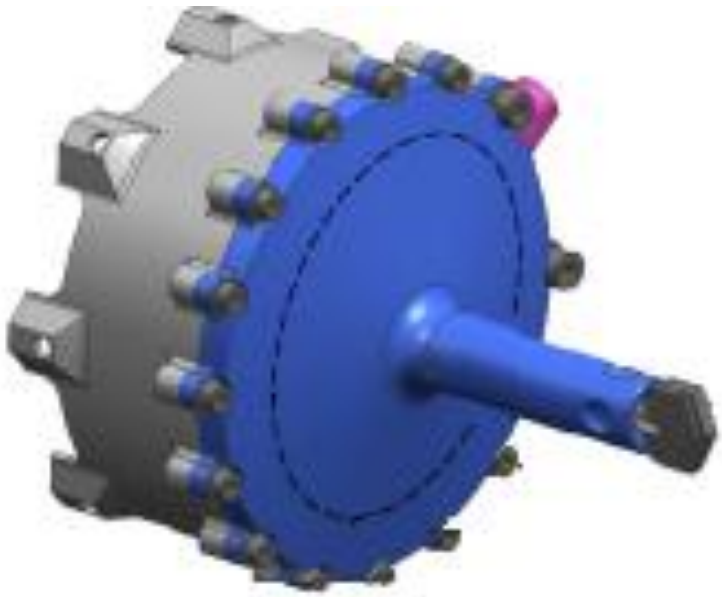

Figure 55 - Drill Bit Assembly, CAD Model

There are a total of four of these detents in the shaft that act as the interface between the drill bit assembly and the BitBox

This interface is detailed further as the ball lock bit restraint in Figure 56 that better shows the complete interface between the drill bit assembly and the BitBox.

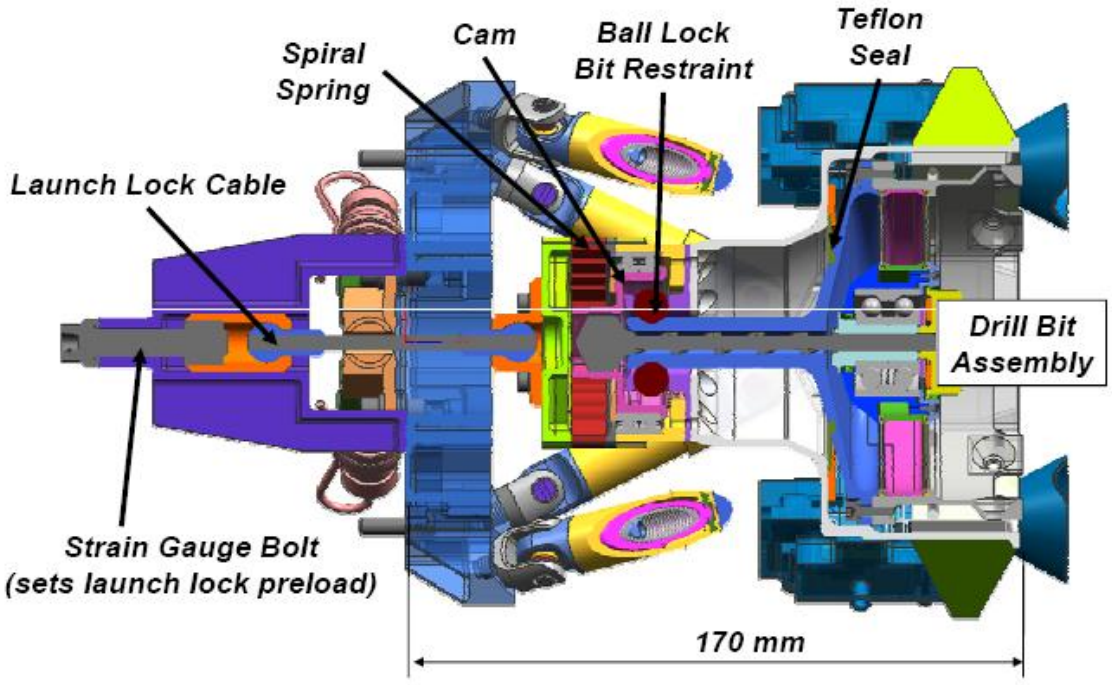

Figure 56 - BitBox, CAD Model Section View

4.1.3 INTERFACE 3 – DRILL BIT ASSEMBLY TO ROBOTIC ARM

There is actually a dual–interface between the drill bit assembly and the robotic arm of the Rover. These two interfaces are depicted in Figure 57.

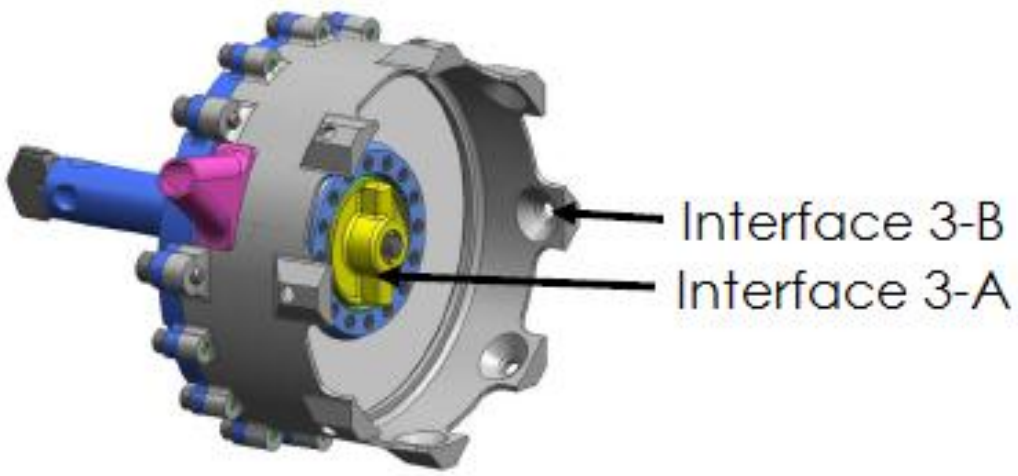

Figure 57 – Interface, Drill Bot Assembly to Robotic Arm

Interface 3-B, also called the "Chuck Interface," are ball detents (8 total) that allows the drill bit assembly to mount to the robotic arm and become a rigid assembly. With interface 3-B being a fixed interface, and with rotational motion still needing to be achieved between from the robotic arm to the drill bit assembly, interface 3-A is the dynamic interface also called the "Spindle Interface". This allows torque from the robotic arm to

be passed to the drill bit assembly and causes the drill bit to rotate with respect to the drill bit assembly.

These two interfaces have their respective mating features on the robotic arm that are recognized in Figure 58.

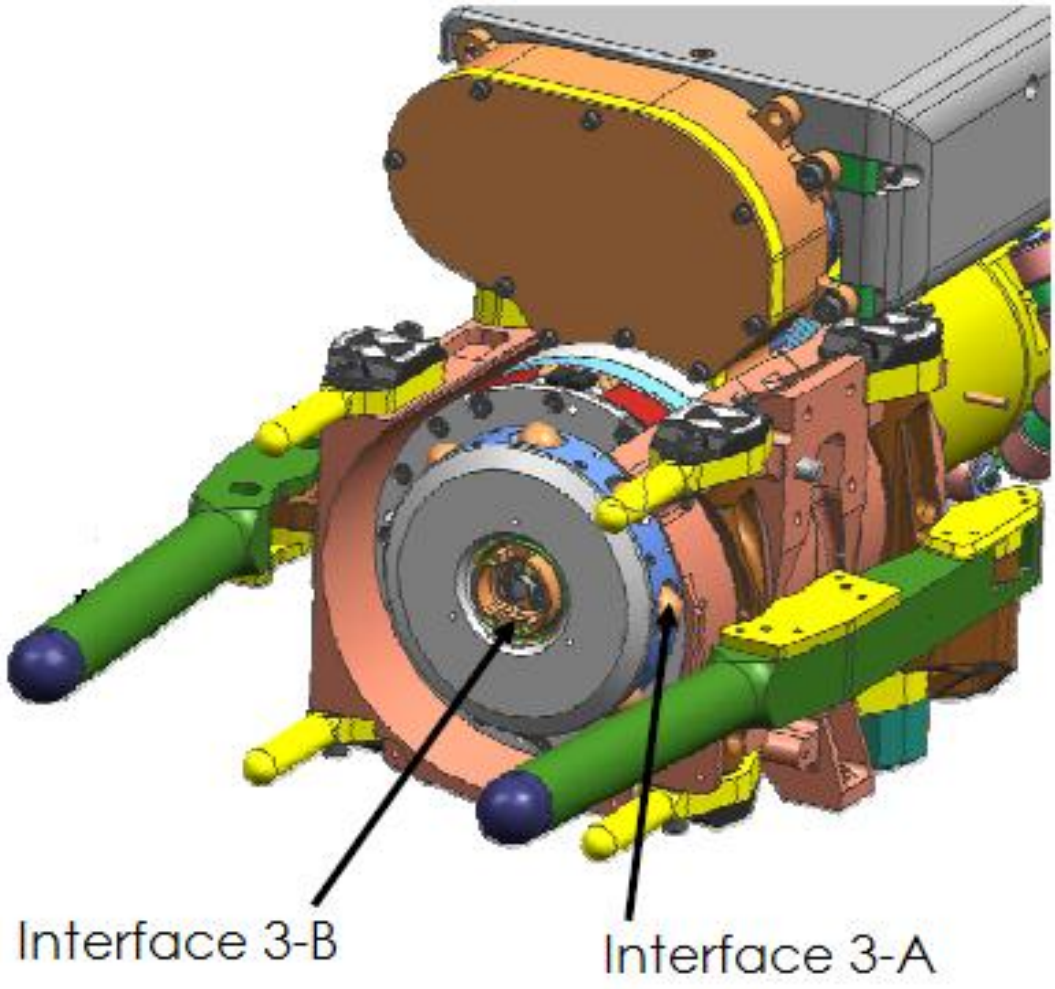

Figure 58 - Interface, Robotic Arm to Drill Bit Assembly

4.2 ROBOTIC ARM ACCESS

The robotic arm of the Rover is able to guide the drill bit to within 2 degrees of accuracy in a worst case situation. The positions and orientations of the BitBoxes must be within the workspace, or the reachable volume of the robotic arm. This can be verified in a variety of manners including trig, MatLab, or Euler Angles, but once there is a fully operational CAD model, the arm can simply be told what position to go to and if it is within the angular ranges then it will go dock accordingly. If not, an error will be displayed stating that it is violating its angular restraints.

4.2.1 BITBOX 1

Figure 59 shows the robotic arm docking with BitBox 1. This view is from underneath the Rover looking upward.

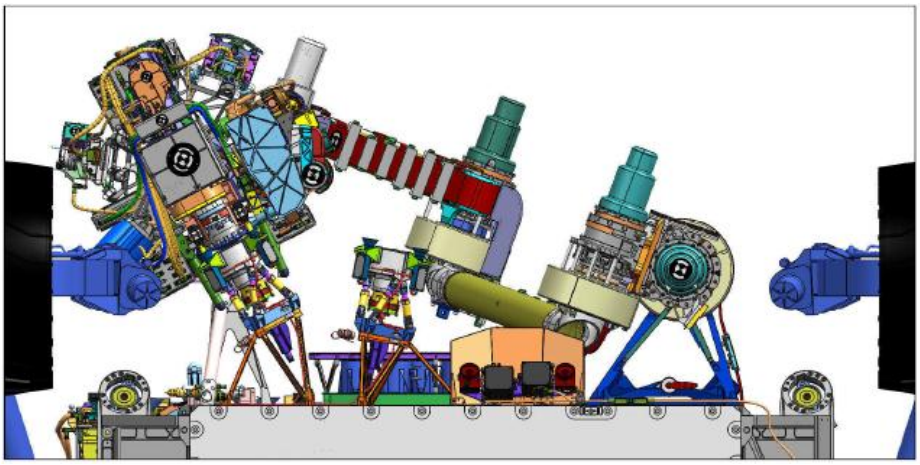

Figure 59 – Turret Access, BitBox 1, Bottom View

This is displayed from a more isometric standpoint in Figure 60.

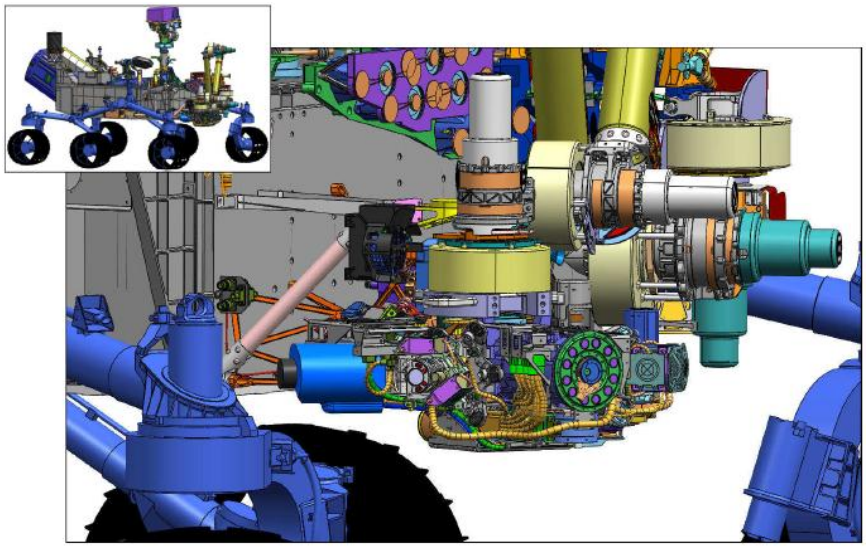

Figure 60 – Turret Access, BitBox 1, Isometric View

4.2.2 BITBOX 2

Similarly, for BitBox 2 the robotic arm can be seen docking from underneath the Rover looking up in Figure 61.

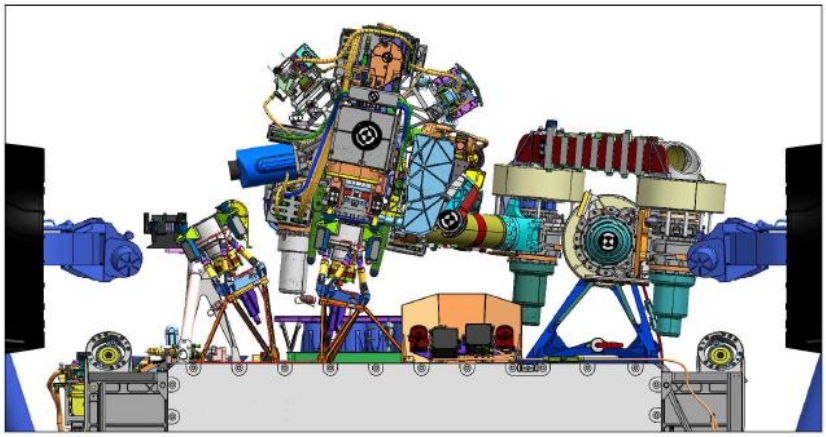

Figure 61 – Turret Access, BitBox 2, Bottom View

This docking is shown from a similar isometric view in Figure 62.

Figure 62 – Turret Access, BitBox 2, Isometric View

4.3 PROCEDURE

This section depicts the successful robotic arm docking and exchange of a new replacement drill bit assembly from a BitBox. The procedure begins by orienting the robotic arm through the use of controlling the degrees of freedom of the joints. This is controlled by internal software where the current position of the robotic arm is known and the final position of the robotic arm has been predetermined in spatial and angular coordinates. The software then controls the rotational joints of the robotic arm to maneuver it into position to acquire a drill bit assembly from a BitBox.

4.3.1 STEP 1 OF 8 – AXIAL ALIGNMENT

The first step is to align the primary axis of the drill bit within the BitBox, and the mount barrel for the drill bit on the robotic arm. This is done so that once these are aligned, within two degrees max error. The arm only has to translate in one direction instead of translating and rotating as it engages the BitBox. This is shown in Figure 63.

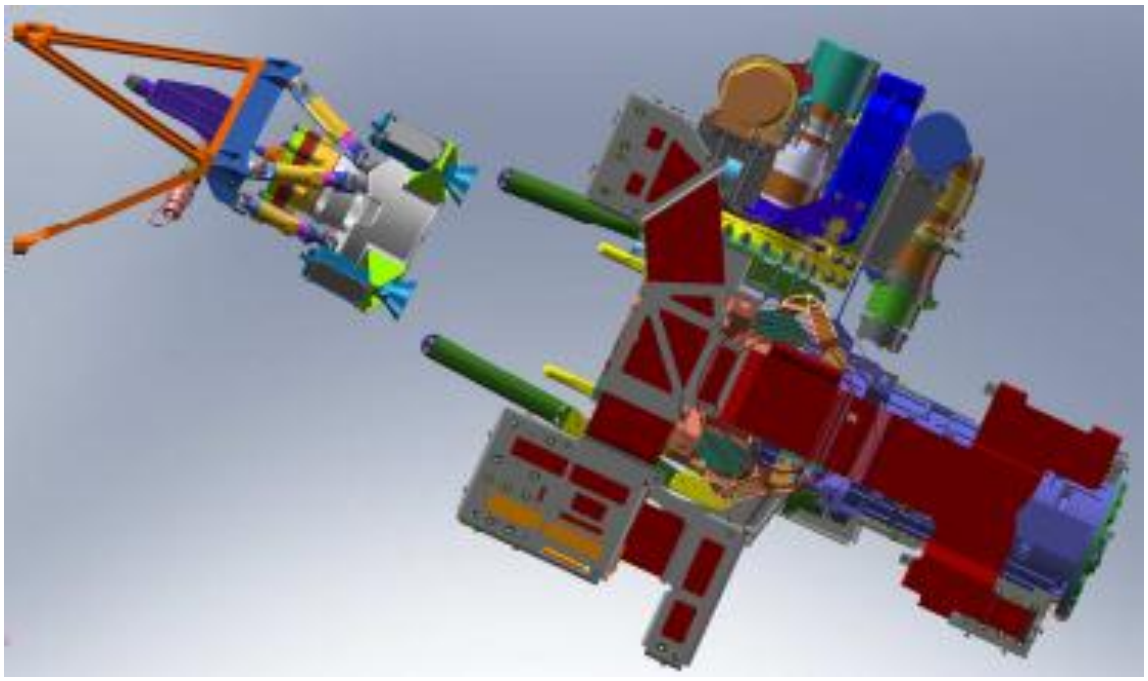

Figure 63 – Axial Alignment of Robotic Arm and BitBox

4.3.2 STEP 2 OF 8 – CONTACT INITIATED

Once axially aligned, the robotic arm translates toward the BitBox until contact is detected between the sensitive alignment posts of the robotic arm and the receptacle cones of the BitBox. The alignment posts have pressure sensors that can detect when this contact is initiated, shown in Figure 64. After contact is made, it is the BitBoxes' responsibility to complete the precision alignment that is required.

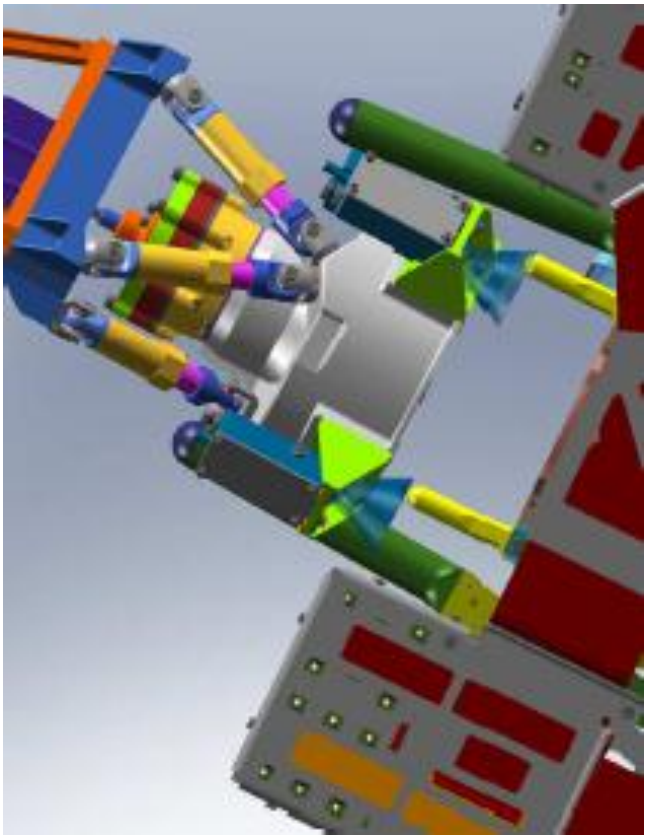

Figure 64 - Robotic Arm Contacts BitBox

4.3.3 STEP 3 OF 8 – BITBOX AUTOALIGN

Once contact is initiated between the robotic arm and the BitBox, the robotic arm then continues to move toward the BitBox only translating along the drill axis. The alignment posts then travel down the inside of the receiver cones and in doing so force the hexapod structure of the BitBox to complete the final alignment. The spring loaded struts compress and extend depending on what is required in order to get the replacement drill bit assembly aligned to the check portion of the robotic arm. Figure 65 shows the initiation of contact between these posts and cones.

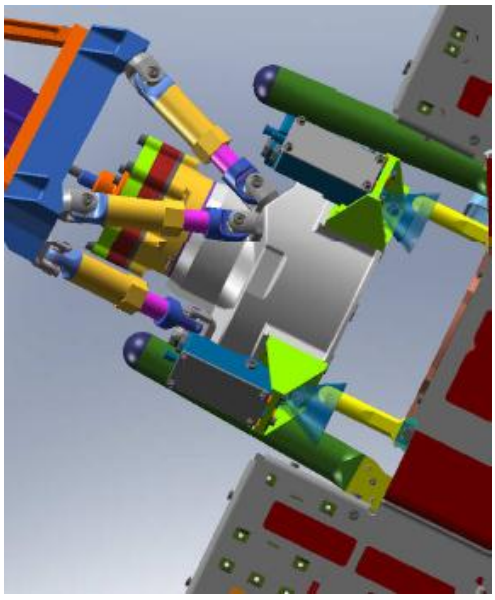

Figure 65 – Auto-Alignment of BitBox to Robotic Arm

4.3.4 STEP 4 OF 8 – CONTACT SWITCHES ENGAGED

Once the BitBox becomes aligned with the robotic arm, the same alignment posts then contact micro-switches at the vertex of the conical receivers. In order to inform the Rover's onboard computer that the robotic arm is now in place to receive the replacement drill bit assembly, three of the four micro-switches must be engaged. Figure 66 shows one of the four alignment posts contacting the micro-switch post thereby closing the circuit.

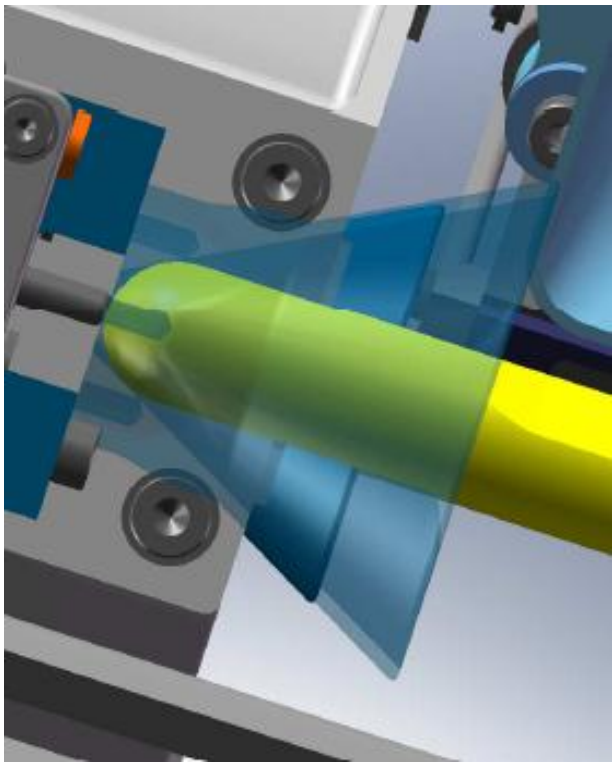

Figure 66 – Robotic Arm Engages BitBox Contact Switches

4.3.5 STEP 5 OF 8 – COMMENCE TORQUE COUPLING

Following the successful micro-switch tripping, the robotic arm is then instructed by the on-board computers to begin the engagement sequence. This involves the chuck-spindle portion of the robotic arm to extend forward into the BitBox to acquire the replacement drill bit assembly. During this, the BitBox and the main body of the robotic arm stays fixed to maintain contact with the switches. Should the alignment post come disengaged with the micro-switch during the torque coupling procedure, the system automatically goes into an abort procedure where the robotic arm moves away from the BitBox until all the micro-switches are disengaged and then it attempts realignment.

This step is depicted as a before and after in Figure 67. The picture on the left shows the chuck-spindle inside of the robotic arm while the picture on the right shows the same chuck-spindle protruding outward to capture the replacement drill bit assembly from the BitBox.

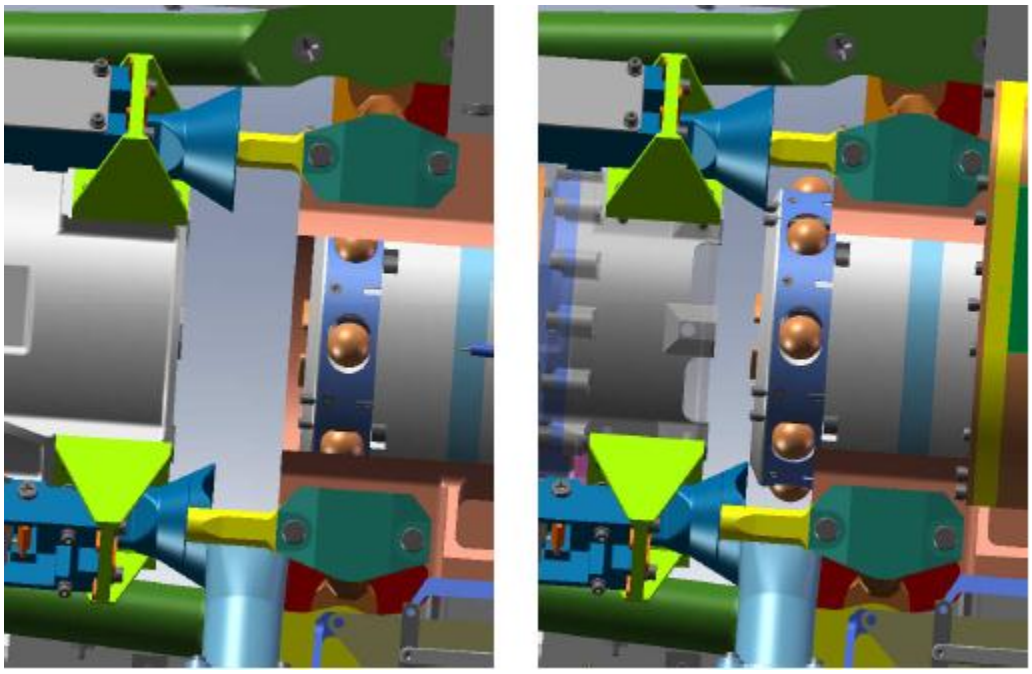

Figure 67 – Chuck Spindle Translating Outward

4.3.6 STEP 6 OF 8 – ROBOTIC ARM CAPTURES DRILL BIT ASSEMBLY

In order for the robotic arm to successfully capture the replacement drill bit assembly, there are two interfaces that must be accomplished. These are interfaces 3-A and 3-B, as detailed in section 4.1.3, and depicted in Figure 68.

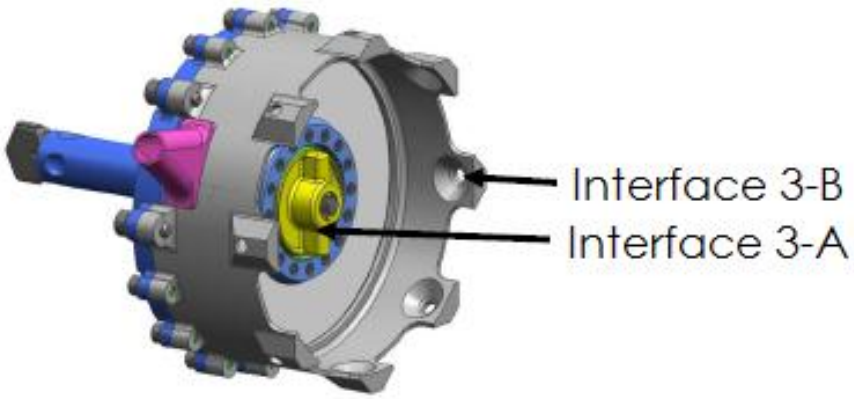

Figure 68 - Robotic Arm Interfaces on the Drill Bit Assembly

Interface 3-A must be achieved first and is the torque-coupling from the robotic arm to the drill bit assembly. This allows the rotational motion to be transferred between the two. Interface 3-B must be achieved next and this creates the rigid connection between the robotic arm and the drill bit assembly. This is done by engaging the eight circumferential balls of the

chuck-spindle outward into the receiving detents of the drill bit assembly. This motion is accomplished through the use of a wave-cam that rotates and drives the balls into place through the use of a wave profile. This is displayed in Figure 69 as a cross-sectional view of the wave-cam. The wave-came is shown in this configuration tangentially pressing the eight balls outward into the receiving detents of the drill bit assembly.

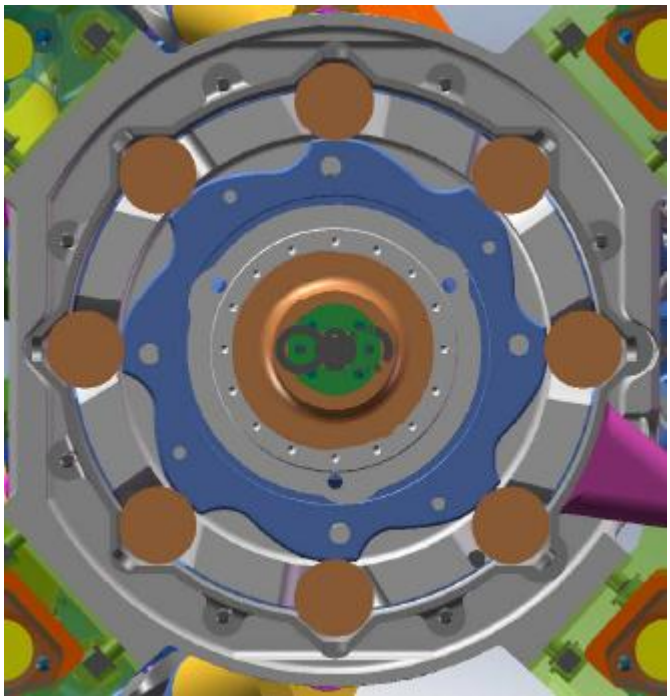

Figure 69 – Wave Cam Locking Drill Bit Assembly to Robotic Arm

The robotic arm and the replacement drill bit assembly are now rigidly and rotationally connected and ready to be removed from the BitBox.

4.3.7 STEP 7 OF 8 – BITBOX RELEASES DRILL BIT ASSEMBLY

This is the last step for the BitBox and works in a similar but opposite fashion to the previous step. Currently the replacement drill bit assembly is rigidly connected to both the BitBox and the robotic arm. The BitBox must now disengage this connection. This is done by rotating a square-cam within the BitBox that releases four balls from detents in the drill bit assembly.

This action is shown in the cross-sectional view in Figure 70. The picture on top shows the balls engaged into the detents of the drill bit assembly because the square profile of the cam has them pressed into this position. The square-cam then rotates 45 degrees, pictured on bottom, so that the balls are thereby released from the detents and translate radially outward into the corners of the cam. The drill bit assembly is now free from the BitBox.

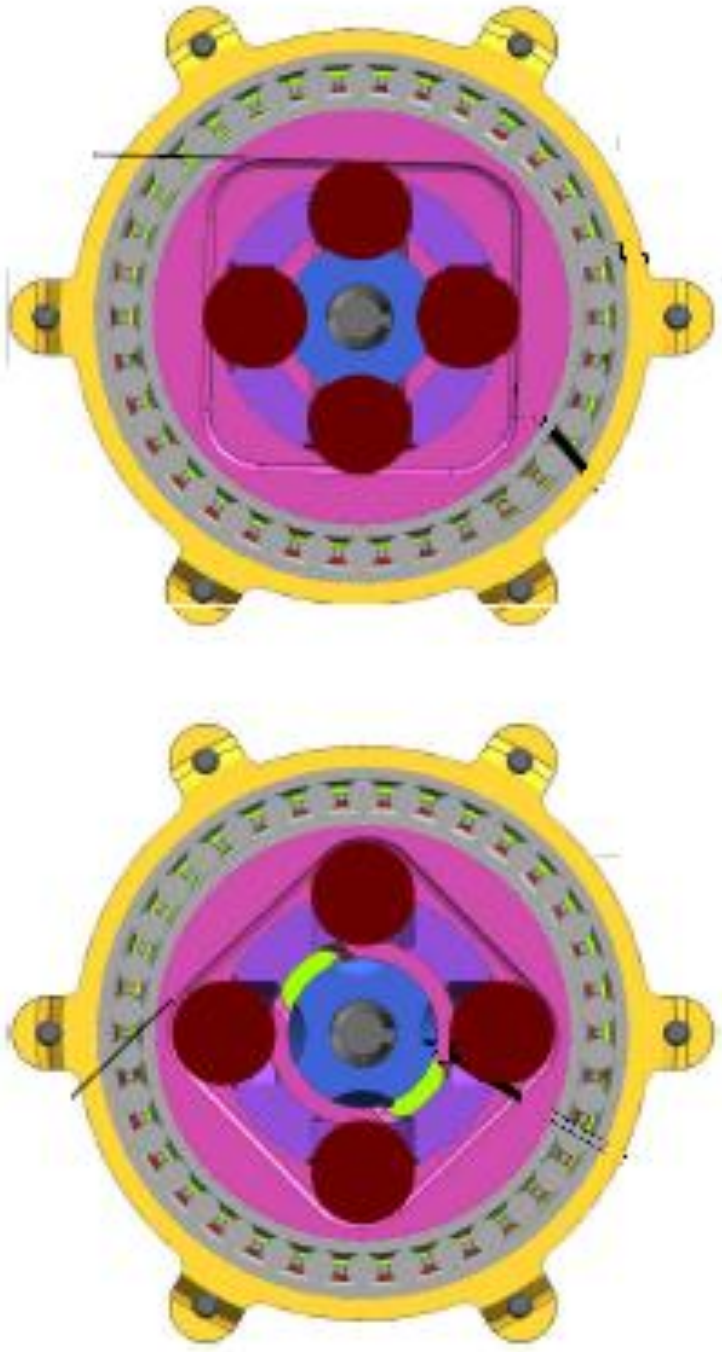

Figure 70 – BitBox Unlocking of the Drill Bit Assembly

4.3.8 STEP 8 OF 8 – EXCHANGE COMPLETE

Once the BitBox cam has released the replacement drill bit assembly to the robotic arm, the exchange is now complete. The only step left to do is to have the robotic Arm pull the drill bit assembly out of the BitBox so that it can begin using it as a tool. This final step is shown in Figure 71, which shows this drill bit assembly firmly affixed to the robotic arm.

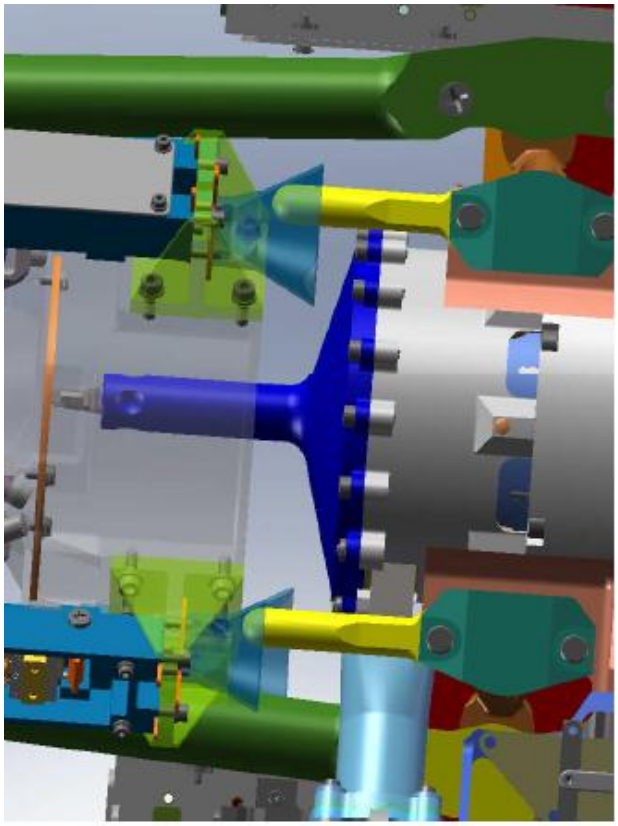

Figure 71 – Drill Bit Assembly on the Robotic Arm

CHAPTER V: SUMMARY AND CONCLUSIONS

In summary, a great deal of mechanical design went into the BitBox for the MSL Rover. This was done iteratively by designing the components with computer-aided design and then optimizing those designs with finite element analysis. The goal of this thesis was to document and illustrate the design process, beginning with an overview of the purpose for designing such am assembly. With the functionality established, the thesis then details the individual parts and mechanisms that, when combined, accomplish the objectives of removing and replacing a drill bit assembly. The next chapter discusses how NASTRAN was used to validate the designs. By using finite element analysis, the parts could be refined to strengthen areas of concern, or reduce them to save mass. With the BitBox design and analysis complete, the thesis then illustrates the key interfaces of the BitBox and illustrates the procedure.

In conclusion, the resulting BitBox proved to function as intended, and two BitBoxes were added to the MSL Rover rather than one as originally planned. Variations of the BitBox design could be used for other robotic missions that utilize a robotic arm, both on terrestrial planets as well as in deep-sea operations.

Figure 72 - BitBox's Shown on First Released Photo of MSL on Mars

Figure 72 shows the 2 BitBoxes in the field of view of the HazCam on MSL. They are shown in the top-right corner with one being more prominent than the other. This figure was the first released photo by NASA-JPL of MSL on Mars with the intention of showing the shadow of MSL with Mt. Sharp in the background. I right away recognized the distinct shape of the BiBox's also including in the picture.

REFERENCES

Davis, Jack, Kyle Brown, and Max von der Heydt. "MSL BitBox DDR." NASA-JPL. Pasadena, CA. 21 Nov. 2008. Lecture.

Missions to Mars. Ed. David R. Williams. NASA, 17 Jan. 2012. Web. 19 April 2012. <http://nssdc.gsfc.nasa.gov/planetary/planets/marspage.html>.

Mars. Ed. Heather Hobdon. CosmicElk, 2012. Web. 19 Apr. 2012. <http://www.cosmicelk.net/Mars.htm>.

APPENDIX A: MISSION BACKGROUND

A.1 MARS – OBSERVATIONAL HISTORY

Mars has long been the subject of human fascination. The earliest recorded history is attributed to the ancient Egyptian astronomers and dates back to 1534 BC. They noted that there was a "wandering object" in the night sky. This was of such interest to the ancient Egyptians that Mars was portrayed in the Tomb of Pharaoh Seti I and in the memorial temple dedicated to Pharaoh Ramesses II.

Systematic observations have also been taken by Babylonian astronomers during the Neo-Babylonian Empire (626 BC – 539 BC), by Chinese astronomers beginning prior to the Zhou Dynasty (1045 BC) , and also by the ancient Greeks (beginning in the 7th century BC). The Greeks, initially led by Plato and his most notable student Aristotle, generated orbital models in "The Republic" (circa 380 BC). That work contained the motion of Mars along with that of Saturn, Jupiter, Mercury, Venus, the Sun, and the Moon. The flaw in their orbital model was that it was geocentric, i.e., the Earth was what all of the previously listed bodies revolved about, including the Sun. This geocentric belief went uncontested for 2,000 years until it was eventually superseded by Nicolaus Copernicus who derived a

heliocentric model where the sun is at the center and all bodies in the solar system orbit around it.

About one hundred years after the Copernican Revolution, an Italian scientist, Galileo Galilei, became the first known person to view Mars through a telescope in 1610 AD. This enabled him and fellow astronomers to view the planet and its motion in unprecedented detail. The Dutch astronomer Christian Huygens noted the presence of what appeared to be a polar ice cap. He also calculated the rotation of the planet to be approximately 24 hours (actual rotational period: 24 hours, 39 minutes, 35.244 seconds) and made a rough estimate that the diameter of Mars was about 60% that of Earth. This compares well to the actual value of 53%.

Increased refinement of the specifics of Mars improved greatly with the increase in size and quantity of telescopes throughout the 19th century with the most notable modern observational discovery being the two moons of Mars, Deimos and Phoobs, discovered at the U.S. Naval Observatory in Washington D.C. by Asaph Hall on August 12th and 18th, respectively, 1877.

Figure 73 shows how the depiction of Mars has changed from the early sketches of Christiaan Huygens in 1659, to the depiction of apparent surface canals by Giovanni Schiaparelli in 1888, to the increased refinement of telescopic views from the early 1960's to the Mars Global Surveyor in 2002.

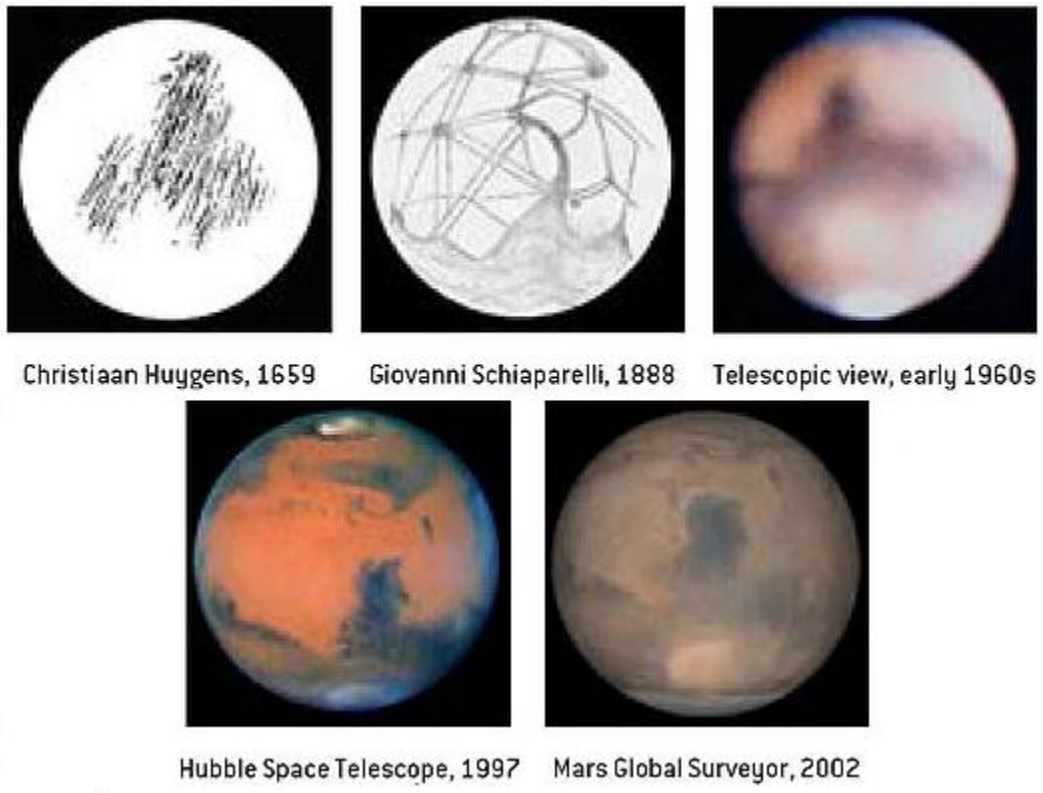

Figure 73 - Observational History of Mars

A.2 MARS – EXPLORATIONAL HISTORY

As a precursor to the manned space race and an undertone to the Cold War, the exploration of Mars began as on aspect in the battle for space supremacy between the Soviet Union and the United States. While putting humans in space and, even more so, landing on the moon was at the forefront of political and media attention, there were many probes sent to Mars as well. These probes fell into 3 categories of increasing mission difficulty:

Flyby: Approach Mars for data and pictures but not obtain orbit; After approach, probe lost to space. Unmanned.

Orbiter: Obtain orbit of Mars for successive data and picture taking. It is difficult to gain orbit because if the probe comes in too shallow, it will skip off the atmosphere and be lost in space. If it comes in too deep it will be swallowed up by the gravitational pull and crash into the planet. Manned or Unmanned.

Lander: Initially enters a planets gravitational pull as an orbiter. After obtaining orbit and stabilizing, enters the planet's atmosphere and lands on the surface. This includes rovers and return missions as well. Manned or Unmanned.

Figure 74 depicts many of the probes sent to Mars all shown in scale with one another. An astronaut can be seen in the bottom right that provides a sense of scale.

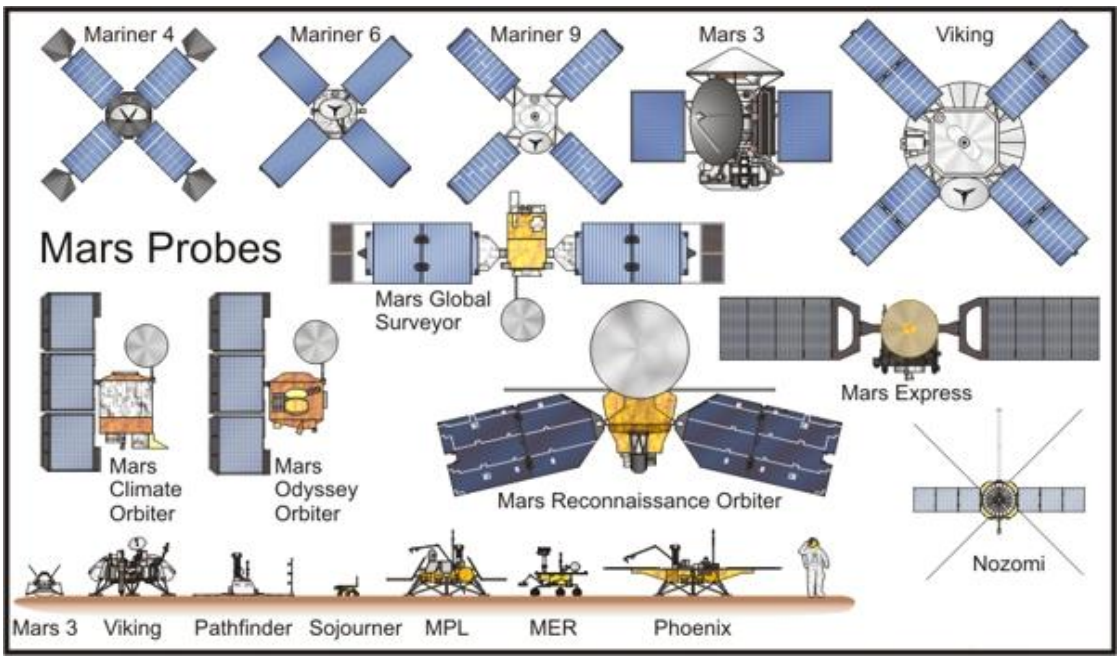

Figure 74 – Explorational History of Mars

The Soviets launched the first 5 missions to Mars all of which failed. The U.S. followed with 2 missions, the first of which, Mariner 3, failed to reach Mars. The second, Mainer 4, shown in Figure 75, became the first ever successful flyby probe to Mars and returned 22 photos of the planet on July 14th 1965.

Figure 75 – U.S. Launched Mariner 4 Orbiter

This U.S. flyby probe success was a small victory in the overall space race. This was coupled with the fact that the Soviet's had launched another attempt at a flyby probe, Zond 2, only 2 days after Mariner 4, however communications were lost en route to the Mars. 5 years later, the U.S. launched 2 additional flyby probes, Mariner 6 and Mariner 7, both of which were successful as well.

The focus then turned to launching a successful orbiter and eventually a lander. Within a week of the U.S. launch success of the Mariner 6 and Mariner 7 probes, the Soviets attempted to launch two potential orbiters, Mars 1968A and Mars 1969B, both of which suffered launch failures. Two years later, in 1971, the U.S. attempted to launch their own orbiter, Mariner 8, but this also had a launch failure. At this point it was increasingly

common that whenever the U.S. launched a probe, the Soviets did as well, usually within weeks of the U.S. probe. While the Soviet probes were typically more ambitious then the American counterparts, their failures indicate that the Soviet engineers might have rushed incomplete designs to the launch pad. This is seen again in that just weeks after the Mariner 8 probe by the U.S., the Soviets launched two identical Orbiter/Lander combinations that they called Mars 2 and Mars 3 shown in Figure 76.

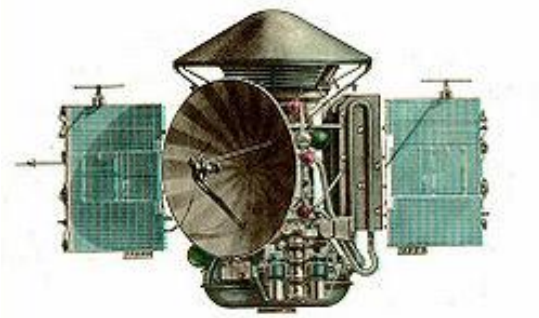

Figure 76 - Soviet Mars 2 & 3 Orbiter/Lander

While both landers failed, the orbiters were semi-successful. This marked the first time a man-made object obtained orbit around Mars, thus becoming an artificial satellite for the planet. This marked both the greatest and last success for the Soviet Mars space program. In 1973 they would go on to launch two additional orbiters, Mars 4 and Mars 5, and two additional landers, Mars 6 and Mars 7, all of which failed at varying

stages of the trip. On the heels of these Soviet failures, in 1975 the U.S. launched two orbiter/lander combinations called Viking 1 and Viking 2, shown in Figure 77.

Figure 77 - U.S. Launched Viking 1 & 2 (Lander Shown)

Both missions were successful and marked the first time a man-made object successfully landed and operated on the surface of Mars. This was also the end of the space race portion of the cold war, which led to a decade long hiatus from further Mars exploration.

In 1988 the Soviets launched two ambitious orbiter/lander probes called Phobos 1 and Phobos 2. The difference between the two orbiters was that the Mars orbiter was to release a secondary probe that would be a

lander for the Martian moon Phobos. While both orbital probes were successful, both landers failed. This marked the last attempts by the Soviets to send probes to Mars as their space program, and country, dissolved in 1991. While the Soviet program halted, the U.S. launched the orbiter Mars Observer in 1992, but communications were lost before reaching Mars. As a follow up, in 1996 the U.S. launched the Mars Global Surveyor which was immensely successful and operated for a decade in orbit around Mars. Also in 1996, the U.S. launched the Mars Pathfinder, which successfully landed on the fourth of July 1997. Around this same time, the newly formed Russian Space Agency launched Mars 96, an orbiter and lander probe, which failed during launch.

After decades of competition between the U.S. and the Soviet Union, the Japanese launched their own Orbiter, Nozomi, in 1998 and while the launch was a success, the probe did fail to enter orbit. However, this did mark the first time a country not involved in the space race successfully launched a probe to Mars. Toward the end of the millennium, the U.S. had two more launches, both of which failed. In 1999, the Mars Climate Orbiter crashed in the Martian atmosphere and later that same year the Mars Polar Lander also crashed. This was followed two years later by the U.S. success of the Mars Odyssey orbiter. The next two launches were by a

newcomer to Mars exploration, the European Space Agency, or ESA, which at the time of the launches, was comprised of 15 European countries. In 2003 the ESA launched the Mars Express orbiter which was a complete success. On board this orbiter was also a lander called Beagle 2 which was successfully deployed, but contact was lost prior to landing. Around this same time, the U.S. launched its two most notable Rovers, shown in Figure 78. MER-A (Spirit) and MER-B (Opportunity) were both launched and successfully landed on the red planet where they both performed far longer than what their operational design was intended for.

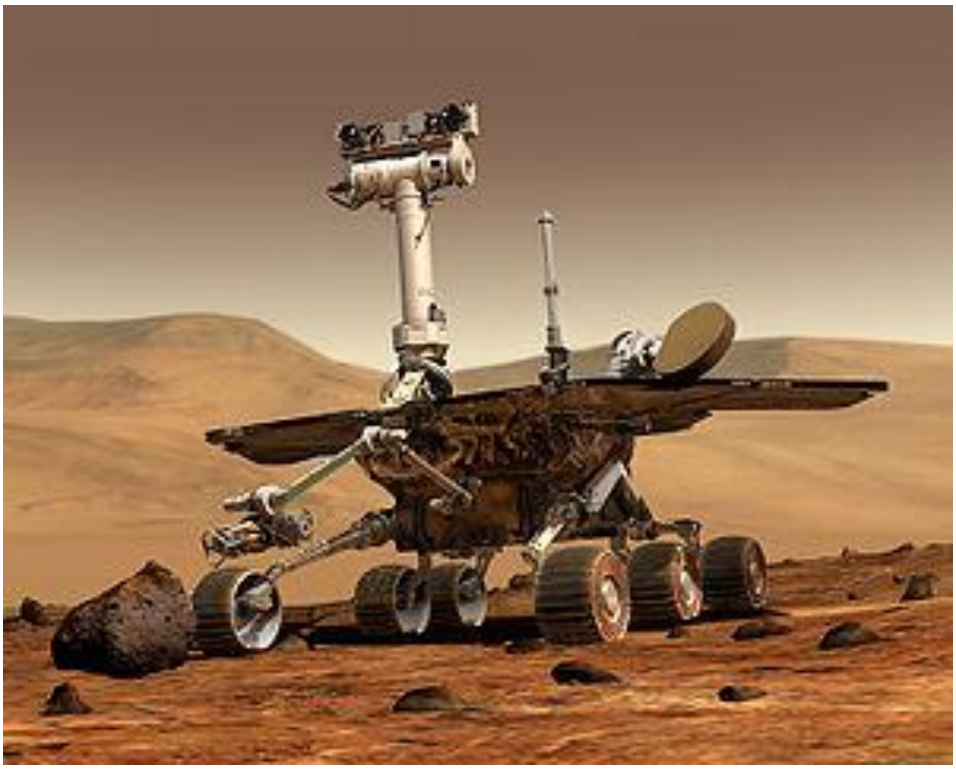

Figure 78 - U.S. Launched MER-A & MER-B Rover

The U.S. then went on to launch an additional orbiter, the Mars Reconnaissance Orbiter, in 2005 and the Phoenix Mars Lander in 2007. Both of these were also successful. In 2011, there were two launches to Mars. The first was by the Russian Space Agency called Fobos-Grunt, which in the spirit of their Soviet predecessors was a very ambitious Phobos sample return mission. However, the probe never made it out of Earth orbit. The most recent launch, and the focus of what this thesis pertains to, is that of the Mars Science Laboratory, shown in Figure 79.

Figure 79 – Mars Science Laboratory Rover

This was successfully launched on November 26th, 2011 and successfully landed on August 6th, 2012 after its eight and a half month journey traveling at approximately 71,000 miles per hour relative to the sun.

Figure 80 – Liftoff of MSL on November 26th 2011

Table 2 - Chronological History of Mars Exploration

Country	Mission	Launch Date	Mission	Result
	Marsnik 1	10 Oct 1960	Flyby	Failed
	Marsnik 2	14 Oct 1960	Flyby	Failed
	Sputnik 22	24 Oct 1962	Flyby	Failed
	Mars 1	1 Nov 1962	Flyby	Failed
	Sputnik 24	4 Nov 1962	Lander	Failed
	Mariner 3	5 Nov 1964	Flyby	Failed
	Mariner 4	28 Nov 1964	Flyby	Success
	Zond 2	30 Nov 1964	Flyby	Failed
	Mariner 6	24 Feb 1969	Flyby	Success
	Mariner 7	27 Mar 1969	Flyby	Success
	Mars 1969A	27 Mar 1969	Orbiter	Failed
	Mars 1969B	2 Apr 1969	Orbiter	Failed
	Mariner 8	9 May 1971	Orbiter	Failed
	Mars 2	19 May 1971	Orbiter/Lander	Success/Failed
	Mars 3	28 May 1971	Orbiter/Lander	Success/Failed
	Mariner 9	30 May 1971	Orbiter	Success
	Mars 4	21 Jul 1973	Orbiter	Failed
	Mars 5	25 Jul 1973	Orbiter	Success
	Mars 6	5 Aug 1973	Lander	Failed
	Mars 7	9 Aug 1973	Lander	Failed
	Viking 1	20 Aug 1975	Orbiter/Lander	Success/Success
	Viking 2	9 Sep 1975	Orbiter/Lander	Success/Success

Table 2 - Chronological History of Mars Exploration (Continued)

Country	Mission	Launch Date	Mission	Result
	Phobos 1	7 Jul 1988	Orbiter/Lander	Failed/Failed
	Phobos 2	12 Jul 1988	Orbiter/Lander	Success/Failed
	Mars Observer	25 Sep 1992	Orbiter	Failed
	Mars Global Surveyor	7 Nov 1996	Orbiter	Success
	Mars Pathfinder	4 Dec 1996	Lander (Rover)	Success
	Mars 96	16 Nov 1996	Orbiter/Landers	Failed
	Nozomi	3 Jul 1998	Orbiter	Failed
	Mars Climate Orbiter	11 Dec 1998	Orbiter	Failed
	Mars Polar Lander	3 Jan 1999	Lander	Failed
	Deep Space 2	3 Jan 1999	Lander	Failed
	Mars Odyssey	7 Apr 2001	Orbiter	Success
	Mars Express	2 Jun 2003	Orbiter	Success
	Beagle 2	2 Jun 2003	Lander	Failed
	MER-A Spirit	10 Jun 2003	Lander (Rover)	Success
	MER-B Opportunity	7 Jul 2003	Lander (Rover)	Success
	Mars Reconnaissance Orbiter	12 Aug 2005	Orbiter	Success
	Phoenix Mars Lander	4 Aug 2007	Lander	Success
	Fobos-Grunt	9 Nov 2011	Lander (Return)	Failed
	Mars Science Laboratory	26 Nov 2011	Lander (Rover)	In Transit

A.3 MARS SCIENCE LABORATORY

With the 50th anniversary of launching probes to Mars occurring in 2010, NASA launched the most ambitious probe yet in the form of a Rover the size of an SUV. This rover it called by several names: Mars Science Laboratory, MSL (for short), and also nick-named "Curiosity" With a successful launch on November 26th, 2011, the rover is in transit to the red planet as this thesis is being written. With an expected touchdown date of August 5th, 2012 the journey to Mars is a long and difficult one. However, the journey to get to the launch pad was even more complicated.

Initially given the go-ahead for conceptual design a decade prior to launching, the success of MSL's predecessors, the MER rovers Spirit and Opportunity, led to MSL being given top priority. The MSL program was given a budget of $1 Billion USD with an anticipated launch date in 2009. The majority of the design, build, assemble and test was performed at NASA's JPL location in Pasadena, CA. The detailed design of the various components began around 2005. In the summer of 2008 there was a major push to successfully meet the November 2009 launch date. The project was about two months behind schedules and was also at $1.5

Billion, i.e, 50 % over budget. Several additional setbacks that were found during testing of the various components pushed the schedule back even further and early in 2009 the mission was postponed to launch in November of 2011 instead of 2009. Due to the orbits of Earth and Mars, they are in sync for launching once every two years. During this time, there was major media backlash against the MSL program and NASA in general. One of the major topics that arose was that the rover was to be powered by plutonium-238 radioisotope thermoelectric generators (RTG). This was because the power required to operate this size of a rover was impossible to be obtained using solar panels. This solution was previously, and successfully, used on the Viking 1 and Viking 2 landers in 1976, but the term "Nuclear Powered Rover" began being used to describe MSL. Standard media questioning of safety should the rocket explode on take-off, degraded into comparisons to that of nuclear missiles. This was definitely the low point of the mission.

The two year delay led to successful testing of all the instruments and the schedule maintained such that a November 2011 launch could be achieved. Probably the biggest issue was that the initial $1Billion budget had ballooned to $2.5 Billion, paid for by taxpayer dollars. This number became synonymous when MSL/Curiosity was discussed. Finally, on

November 26th, 2011, 10 years of work by 5,000 engineers, scientists and all the other fields involved successfully launched out of Cape Canaveral, Florida and the bad taste of the budget and schedule was instantly washed away. On news channels that were broadcasting the launch, the talk of the budget went from having negative undertones to positive ones when it was being compared to the cost of the Iraq/Afghanistan war. The comparison was that such a remarkable man-made instrument that employed so many people for a decade did cost $2.5 Billion, but that this was equivalent to the cost of three and a half days of war.

APPENDIX B: BILL OF MATERIALS

Table 3 (extending over this and the following two pages) shows all of the components that were designed or sourced to create the two BitBox assemblies. BitBox 1 and 2 are identical except for their respective structures that mount them to the front panel of the MSL Rover.

Table 3 - BitBox Bill of Materials

	BITBOX 1 QTY	BITBOX 2 QTY
10272710-1 DRILL BIT ASSEMBLY	1	1
10303308-1 BITBOX STRUCTURE 1	1	-
10303308-2 BITBOX STRUCTURE 2	-	1
10301190-1 BIT BOX ASSEMBLY	1	1
10301167-1 BASEPLATE	1	1
10301168-1 STRUT CLEVIS	12	12
10301169-1 STRUT SPACER	24	24
10301180-1 RECEIVER ASSEMBLY	1	1
10301175-1 BITBOX RECEIVER	1	1
10301176-1 TEFLON RING RETAINER	1	1
10301177-1 ALIGNMENT BRACKET	3	3
10301177-2 ALIGNMENT BRACKET	1	1
10301178-1 ALIGNMENT CONE	3	3
10301178-2 ALIGNMENT CONE	1	1
10301179-1 BEARING HOUSING	1	1
10301181-1 BEARING HOUSING	1	1

Table 3 - BitBox Bill of Materials (Continued)

10301182-1	BEARING CLAMP	1	1
10301183-1	CLOCK SPRING	1	1
10301184-1	BOTTOM COVER	1	1
10301185-1	BEARING INNER CLAMP	1	1
10301186-1	BITBOX CAM	1	1
10272750-1	CAM BEARINGS	1	1
10301189-1	TEFLON SEAL RING	1	1
10303303-1	LAUNCH LOCK CABLE RETAINER	1	1
BIT RETAINING BALLS		4	4

10301260	**SWITCH ASSEMBLY**	4	4
10301261-1	SWITCH HOUSING	4	4
10301162-1	SWITCH HOUSING COVER	4	4
10301163-1	SWITCH MOUNT	4	4
10301163-2	SWITCH MOUNT	4	4
10301164-1	SWITCH ROCKER	4	4
10301165-1	SWITCH CONTACT PIN	4	4
10301166-1	SWITCH SPRING PIN	4	4
10301167-1	FELT SEAL	4	4
CSC 11254 SPRING		4	4
9hm30-rel-pgm Microswitch		4	4
MS 16555-22 ROCKER PIVOT PIN		4	4

10301170-1	**STRUT ASSEMBLY**	6	6
10301171-1	LOWER STRUT END CAP	6	6
10301172-1	STRUT HOUSING	6	6
10301173-1	STRUT ROD	6	6
10301174-1	UPPER STRUT END CAP	6	6
10301188-1	STRUT PIN	12	12
SKF-GE-4E	SPHERICAL BEARING	12	12
SMALLEY EH-12-S02	SPIRAL RETAINING RING	12	12
CUSTOM	STRUT SPRING	6	6

10303310-1	**LAUNCH LOCK ASSEMBLY**	1	1

Table 3 - BitBox Bill of Materials (Continued)

10207827-1	CABLE CUTTER	1	1
10303304-1	BALL SHANK HOUSING	1	1
10303305-1	LAUNCH LOCK BRACKET	1	1
10301187-1	LAUNCH LOCK CABLE	1	1
DS136-31-16	STRAINSERT PRELOAD BOLT	1	1
NSI AND BOOSTER MODULE		2	2

- Off the Shelf items shown in orange text
- All fasters omitted from this Bill of Materials

APPENDIX C: DESIGN DRIVERS

There were several design drivers that had to be addressed during the brainstorming part of the initial design. These design drivers were provided by systems engineers as to what capabilities the BitBoxes needed to function under. There were eight design drivers that pertained to the loads that the BitBox is expected to see, the tolerance of alignment, the mechanism life cycle, and other physical characteristics of the BitBox. These are detailed in Table 4 on the following page.

Table 4 - BitBox Design Drivers

Design Driver Line Number	Design Driver Description
BitBox DD1	Drill Bit Assembly (DBA) must be retained in BitBox against 35-G launch loads and 8.5-G mobility loads
BitBox DD2	Robotic Arm misalignment (12mm lateral, 2 deg angular) during docking requires 6-DOF compliance in BitBox to properly align Drill Chuck with Drill Bit Assembly
BitBox DD3	Robotic Arm provides up to 300 N of axial force for docking
BitBox DD4	Packaging on rover front panel is driven by limited turret access
BitBox DD5	BitBox must sense when Robotic Arm has docked and is acquire in position to Drill Bit Assembly
BitBox DD6	Drill Spindle rotational position is unknown during Bit Exchange
BitBox DD7	Drill Bit Assembly must be released from BitBox with <1.8 N-m of torque from drill bit
BitBox DD8.A	Mechanism Life - Stewart Platform struts are repeatedly cycled by mobility loads
BitBox DD8.B	Mechanism Life - All other mechanisms are essentially one-time use